Annual Report
from April 1, 1996 to March 31, 1997
Department of Plasma Research and Department of Fusion Facilities

Naka Fusion Research Establishment
Japan Atomic Energy Research Institute
Naka-machi, Naka-gun, Ibaraki-ken, Japan 311-01

This report provides an overview of research and development activities at Department of Fusion Plasma Research and Fusion Facilities, JAERI, during the period from April 1, 1996 to march 31, 1997. The activities in this period are highlighted by high temperature plasma research in JT-60 and JFT-2M.

The objectives of the JT-60 project are to contribute to the ITER physics R&D and to establish the physics basis for a steady state tokamak fusion reactor like SSTR.

To achieve these objectives, improvements and regulation of the facilities and developments of the instruments were performed. The highlights are as follows. The construction for the divertor modification from the original open type to the W-shaped semi-closed type for improving the particle control was started on February 1997. In the power supply system, the thyristor converter was partially rearranged to increase the plasma current with the high triangularity. The world record of plasma input power 40 MW was achieved by NBI with the beam energy of 90 keV using positive ion source. Also in negative-ion based NBI, the beam output of 18.4 A/350 keV(6.4 MW) with hydrogen and 13.5 A/400 keV(5.4 MW) with deuterium were achieved as the world record. Furthermore, a plasma input power of 3.2 MW/350 keV to JT-60 was realized with the single ion source. In LHRF system, a protection system of the antenna from the arcing was developed by means of detection of the light caused breakdown.

The followings are the results concerning the plasma performance. By extending the operational region of the high β_p H-mode, the world record of the fusion triplet, $n_D\tau_E T_{i0}$ = 1.53×10^{21} keV s m^{-3}, was achieved. It was found that the fusion triplet became maximum in the same region of the safety factor as the ITER operation.

electron density 0.97×10^{20} m^{-3}, the fusion triplet 0.78×10^{21} keV s m^{-3}. The fusion power by D-D reaction was 53 kW, and assuming that the half of the fuel was tritium, the expected fusion output was 10.6 MW. The ratio of the output to the input power becomes 1.05, therefore it can be concluded that the plasma is in an equivalent break even condition. Moreover, in a reversed shear plasma, the highest values of the energy confinement time and the stored energy on JT-60

(1.08 s and 10.9 MJ) were recorded. Generation of radiative divertor, confinement of high energy ions, current profile control by RF current drive and impurity confinement in reversed shear plasmas were investigated systematically.

The poloidal coil system was modified so as to increase the triangularity. As the result an instability driven by the pressure gradient at the plasma edge was drastically suppressed, then a plasma with the confinement improvement factor of more than two and the fusion triple product of 0.27×10^{21} keV s m^{-3} was successfully maintained for 2.6 seconds. Furthermore, by raising the triangularity a full current drive plasma was successfully maintained with high confinement property and high fraction (60%) of the bootstrap current for three times longer than was formally achieved. A driven current of 270 kA was demonstrated by the negative ion based neutral beam injector (N-NBI) for the first time, and a profile of the current was estimated. The current drive efficiency by N-NBI was proved to be better by 1.6 times than that by standard energy (~90 keV) positive ion based NBI.

Objectives of the JFT-2M program are (1) advanced and basic researches for the development of high-performance plasmas for nuclear fusion and (2) contribution to the physics R&D for ITER, with a merit of flexibility of a medium-size device. The modified closed divertor was found to improve compatibility of the H-mode with the dense and cold divertor plasma. In an H-mode plasma, suppression of the density fluctuation was found to occur in a high shear region of the radial electric field. It was demonstrated that the m=2 tearing mode was suppressed by the O-mode ECH for the first time in an elongated plasma. Plasma coupling experiment of the combline antenna for FWCD was carried out in collaboration with General Atomics. Planning of the Advanced Material-Tokamak Experiments (AMTEX) was initiated.

The primary objective of theory and analysis is to improve the physical understanding of the magnetically confined tokamak plasma. Remarkable progress has been made on understanding of physics of the reverse shear plasma, stability properties of ideal MHD, TAE and kinetic ballooning modes. Progress was also made in understanding of VDE mechanism and nature of divertor asymmetry. New Implicit Monte Carlo method is also developed for the analysis of impurity ionization and recombination. Selective He ash exhaust is also demonstrated using OFMC code simulation.

The main focus of the NEXT (Numerical Experiment of Tokamak) project is to simulate tokamak plasmas using particle and fluid models on the developing technology of massively parallel computers.

Keywords: Fusion Research, JAERI, JT-60, JFT-2M, DIII-D, Plasma Physics, Fusion Engineering, ITER, ITER-EDA, Fusion Reactor Design, Annual Report

---

Editors: Shimizu M.(chief), Ide S., Matsukawa M., Kurihara R., Koizumi K., Takahashi I.

Contents

I. JT-60 PROGRAM

Objectives of the JT-60 project are to contribute the ITER physics R&D and to establish the physics basis for a steady state tokamak fusion reactor like SSTR. Significant progress in key physics for ITER and SSTR design has been made in recent JT-60 experiments.

By extending the operational region of the high β_p H-mode, the world record of the fusion triple product, $n_D\tau_E T_{i0} = 1.53 \times 10^{21}$ keV•s•m^{-3}, was achieved. It was found that the fusion triple product became maximum in the same region of the safety factor as the ITER operation.

Optimization of the reversed shear mode, which has been investigated experimentally since FY 1996, in a higher current regime realized a reproducible high fusion performance plasma with high temperature and density. The main achieved parameters of the plasma are as follow; the energy confinement time 0.97 s, the ion temperature 16.5 keV, the electron density 0.97×10^{20} m^{-3}, the fusion triple product 0.78×10^{21} keV•s•m^{-3}, and the fusion power by D-D reaction in the deuterium plasma was 53 kW. Assuming that the half of the fuel was tritium, expected fusion output was 10.6 MW, while the input power was 10.1 MW, then the ratio of the output to the input power becomes 1.05. Therefore it can be concluded that the plasma is in an equivalent break even condition. Moreover in a reversed shear plasma, the highest values of the energy confinement time and the stored energy on JT-60 (1.08 s and 10.9 MJ) were recorded. Generation of radiative divertor, confinement of high energy ions, current profile control by RF current drive and impurity confinement in reversed shear plasmas had been investigated systematically.

Based on the result in FY 1995 the poloidal coil system was modified so as to increase the triangularity for better plasma stability. As the result an instability driven by the pressure gradient at the plasma edge (giant ELM) was drastically suppressed, then a plasma with the confinement improvement factor of more than two and the fusion triple product of 0.27×10^{21} keV•s•m^{-3} was successfully maintained for 2.6 seconds. Furthermore, by raising the triangularity it was succeeded to maintain a full current drive plasma which had high confinement property and high fraction (60%) of the bootstrap current for three times longer than that formally achieved. These achievement are important to determine an operational mode and a plasma shape of a steady state fusion reactor.

Experiments of the negative ion based neutral beam injector (N-NBI) had progressed to reach the power of 3.2 MW/unit (80% of the full spec) and the beam energy of 400 keV (80% of the full spec). A driven current of 270 kA was demonstrated by N-NBI for the first time, and a profile of the current was estimated. The current drive efficiency by N-NBI was proved to be better by 1.6 times than that by standard energy (~90 keV) positive ion based NBI. It was also shown that behavior of beam ions was consistent with the classical theory.

1. Operation and Machine Improvements

In FY 1996, a total of 1,964 pulses were run during the period of 9-cycle operations and wall conditioning. The total number of shots carried out for the past twelve years amounts to 22,148 as shown in Fig.I.1-1.

In mid-April, a few carbon fiber composite (CFC) tiles broke away from the divertor in the experimental campaign aiming at high-Q_{DT} plasma performance. These divertor tiles were replaced by new ones in a shutdown period of May. In this shutdown, various maintenance works including inspection of high pressure gas facilities such as the pellet injector and the NBI cryopump system were performed in JT-60 facilities.

Following this short shutdown, wall conditionings by NBI-heated tokamak pulses and boronization were performed in June. Campaigns of high βp H-mode and negative shear experiments were started from July aiming at obtaining plasmas with high-Q_{DT} performance. In July, the negative-ion based NBI (N-NBI) system was inspected by the STA. Although a few CFC tiles were broken away from the first wall in experiments with high triangular configuration in mid-September, the repair work of the tiles was done at the succeeding maintenance week and no disturbance was made to the experiments started from late in September. After that, the campaign of negative shear experiments was conducted and break-even condition was achieved and the effective energy multiplication factor Q_{DT} = 1.05 was obtained on October 31.

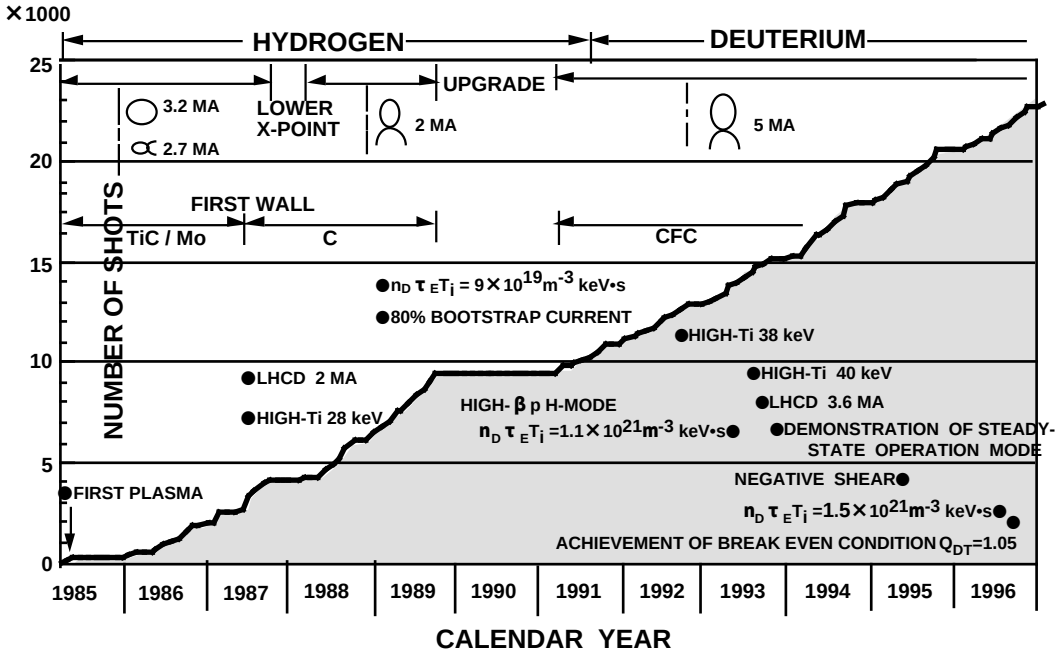

Fig.I.1-1 Progress in JT-60 operation

Annual maintenance of the JT-60 facilities were performed from November through December in 1996. In this shutdown, the cooling pipes in the toroidal field coils were inspected, and a detailed inspection of the motor generator for the toroidal field power supply was also carried out. The operation restarted in mid-January 1997 and experiments with hydrogen continued till

early in February. In this period, the N-NBI beam of 320 keV, 3.2 MW with hydrogen was successfully injected into JT-60. In mid-February, a shutdown started for the modification of the divertor from open-type to the W-shaped semi-closed pumped divertor. This modification is scheduled to finish in May 1997. In this period, a detailed inspection of the motor generator for the poloidal field power supply was also performed.

In spite of many troubles caused by aged deterioration of facility components and exploitation of new areas in core-plasma performance, JT-60 was satisfactorily operated throughout the year. The database obtained in the operation and maintenance was arranged and made useful for maintenance plan and measures for improving the aged deterioration of the facilities.

1.1 Tokamak

1.1.1 Operation and maintenance of the JT-60 machine

Operation and maintenance of the JT-60 machine have been carried out almost on schedule.

In relation to toroidal field coil (TFC), the inspection of TFC have been made two times, in May and in December, 1996 during the regular shutdown. Air tightness test was carried out for all cooling pipes, and inside of 16 cooling pipes selected were observed by fiber scope. Any deterioration of the cooling pipes were not found. Temperature measuring system, which can serve for safety operation of TFC-9 with a damaged coil turn, has been modified to strengthen the monitoring functions by installing the work station.

Three types of plasma configurations, namely, standard, high elongation, and high triangularity plasma configurations have been operated by changing the combination of the poloidal field coils (PFC). Feeder temperature has been measured for the high triangularity plasma configuration because of its excess temperature from the rating during operation.

The pellet injection system has been operated for studies for disruption with injection of Ne pellets and of the plasma confinement improvement with deuterium pellet injection.

The 8th boronization was performed in April 1996 by using boronization system.

As regard the troubles, first wall tiles fell off two times. One was prototypal tile due to lack of strength at P1 section in April. Another was happened at upper of inboard tiles at P14 section in September. It was caused by excessive heat load by the high triangularity operation. In both troubles, damaged tiles were replaced immediately and we could restart the operation of JT-60 in the next week. The vacuum leakage was occurred at P18 section due to damage of the diagnostic window. Electrical insulation was become to wrong due to damage of the honeycomb plate at NBI in P17 section. These troubles were rapidly repaired and there were not so much effect to operation schedule.

From February to June, modifications of the divertor, the vacuum exhaust facility, the gas injection facility and the pellet injection facility have been performed. In the vacuum exhaust facility,

turbo molecular pumps were replaced to advanced levitated type for being free from charging radioactivity and for reducing maintenance fee. In the gas injection facility, the injection port was increased from two to six. This relocation of gas injection port is expected to improve plasma confinement, progress in study of radiation loss and helium ash exhaust. The pellet injection facility will replace from air-gun pellet injector to centrifuge pellet injector. This modification realize continuative pellets injection and will be expected to maintain high density plasma. As the other modification, differential exhaust system for electromagnetic diagnostics and leak test stand for D_2 have been modified to remotely-controllable system and the check booth of JT-60 was also installed.

1.1.2 Modification of divertor

Modification from open divertor to W-shaped pumped divertor was completed almost on schedule. This construction started end of February in 1997, and was completed in May.

The W-shaped divertor consists of inclined targets, dome and inner, outer baffles. This W-shape configuration was adopted to realize radiative divertor plasma for reduction the heat load to the divertor targets and good H-mode confinement simultaneously. Designed maximum plasma current and toroidal magnetic field are 3MA and 4T, respectively. Maximum net heating power is 30MW. High radiative steady operation with 70% radiation loss of the net heating power and low radiative short-pulse operation with 30% loss are assumed. So, heat flux to the divertor targets is expected to be $5MW/m^2$ x 10s - $10MW/m^2$ x 4s.

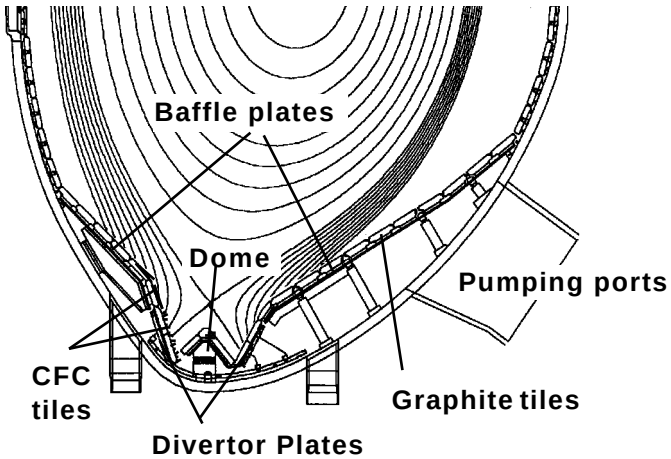

Fig.I.1.1-1 Structure of W-shaped

The structure of this W-shaped divertor, which is shown in Fig.I.1.1-1, is segmented toroidally and poloidally. Divertor and dome are composed of 125 toroidal-segments. Inner and outer baffles consist of 72 blocks. Materials of these structure are mainly stainless steel (SUS-316) and Inconnel (Inconel-625) with low cobalt content. Inconel was used for the baffle plates to avoid thermal stress during baking of vacuum vessel, because vacuum vessel was made of Inconel. Stainless steel was used for the divertor base plate, since the divertor was fixed to the present cooling basement, which was made of stainless steel. Gaps between adjacent components are gas-sealed by insert-sliding mechanism. Sliding parts are electrically insulated by sprayed ceramic coating to avoid arcing. CFC tiles are used for the divertor targets, top of the dome and baffle tiles at the divertor throat. For other parts, isotropic graphite tiles are used. These tiles were designed in consideration of strength for halo current and

orientation of carbon fiber for heat load.

This W-shaped divertor has inertial cooling system. Even without water cooling, however, high power operation is possible with intervals of 20 minutes. Divertor tiles tapered with edge level difference of 0.5mm were fabricated to avoid heat concentration to the edge. These tiles were aligned with good accuracy of assembling. Cryo-pumps of three NBI heating units are used as a divertor pumping system. Effective pumping speed at the pumping entrance in the divertor region is estimated to be about 40 m^3/s. This pumping speed can be changed during a discharge by fast shutter valves of the NBI cryo-pumps for active control of particle exhaust. The leakage conductance of the baffles is estimated to be 1/10 - 1/20 of pumping speed.

1.2 Control System

1.2.1 Operation of the control system

The control system constantly works in the JT-60 experiments according to the required schedule. A function was newly developed in this fiscal year to increase shot availability (= shot numbers per day) under the condition that the temperature at the most narrow point of the toroidal field coil conductor with coolant leakage be kept below the limit of the electric insulator material. When the operator completes a next discharge condition set, this function calculates the waiting time for sequence start, so that the coil be cooled down low enough at the next excitation. In addition, in order that the coil safety be guaranteed, this function finally checks whether the temperature at 1 minute before discharge decreases below the allowable level. As the result from its installation to the working system, the availability of JT-60 experiment was increased by 20 %.

Corresponding to the modification of the first wall to a closed divertor type, part of the existing magnetic sensors were moved, and several pairs of magnetic probes were newly installed. Hence, new coefficients of the formulas for calculation of the macroscopic controlled parameter such as plasma major radius, were established using the JT-60 new equilibrium data files.

For the maintenance of the control system, annual inspections were made of the computer system, control boards, and the signal processing system for plasma control in the shut-down period of November and December. The general purpose computer system, containing all of the JT-60 discharge result data, was superseded to a UNIX workstation system, a new data base system, having been developed for two years, was come into operation. The software change for the data handling was smoothly conducted.

1.2.2 Development of a precise long-time digital integrator for magnetic measurements

Magnetic field measurements are indispensable for control and diagnostics of a tokamak plasma. The existing methods for the measurement are (i) integration of time-derivative of magnetic field, and (ii) direct measurements of absolute magnetic field using rotating coils, Hall-element sensors, etc. The latter seems to be incompatible with 14-MeV neutron field, while the former has

a problem of signal drift inevitable in an integrator, and thus it could not work for a long period of discharge (e.g. 1000 s for ITER). We chose the VF (voltage-to-frequency)-UDC (up-down counter) method for the development from the following view points: Its high accuracy is expected equivalent to analog integration. Wider dynamic range is allowed in a large digital accumulator, and drift can be compensated more precisely in a digital system.

The current results of the development are as follows [1.2-1]: (1) Technical causes of drift in the old VF-UDC system for JT-60 were analyzed. A new VF converters, then, have been developed with taking all measures identified in the analysis. (2) The first version of the new VF converter (VF#1) showed small amount of drift for 24 hours in a stand-alone integration test with input short. (3) Conversion linearity of the VF#1 is much improved from 0.027 % FS (the old VF) to 0.002 % FS (VF#1) in the ranges of ±10V and 1±0.5MHz. A dead band width at 0-V input is reduced from a few mV to several tens of micro volts. (4) A new method for drift compensation is being installed in the VF#2, which can suppress the amount of drift with constant speed to several counts for 1000-s integration.

The measurement with the VF-UDC in JT-60 experiments will be conducted in June 1997.

1.2.3 DSP application to fast parallel processing in JT-60U plasma shape reproduction

Recently the experimental observation has been recognized that the full shape reproduction and control is one of the important issues for improving plasma energy confinement performance. The requirements for more sophisticated plasma position and shape real-time control stimulates development of the parallel processing system.

In the methods of plasma shape reproduction, the core computational procedure is to determine the outermost magnetic surface using the flux function [1.2-2]. We adopted a TMS320C40 DSP as a main real-time processor, because this DSP has 6 ports to communicate separately with other DSP's for parallel processing. A newly designed system is composed of 8 nodes of the DSPs, four of which have 32-MB memories [1.2-3]. This system was succeeded to work in parallel, and reproduces plasma shape in real time. The shape identification calculation can

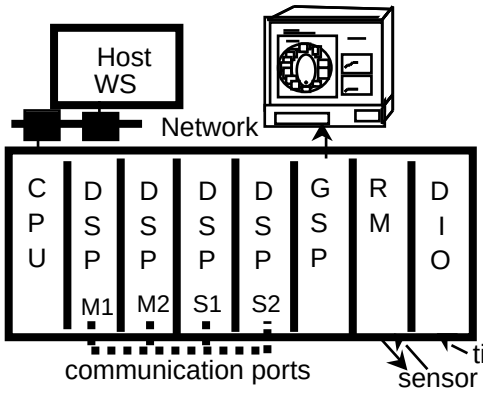

Symbol	Type	Function /Manufacturer
CPU	MVME147	MC68030, 25MHz / Motorola
DSP M1, M2	DSP8040	TMS320C40x2, 40MHz, 2MB/MTT
DSP S1, S2	DSP8044	TMS320C40x2, 40MHz,
GSP	UDC6000TI	Graphics Processor TMS34020, 33MHz / Univision
RM	DSP8230	Digital Input (32 ch) / MTT
DIO	VMIVME5576	Reflective Memory (256kB) / VMIC

Fig.I.1.2-1 Configuration of the improved JT-60U plasma shape reproduction system

be performed at every 25 ms, and the full shape can be drawn at every 50 ms at JT-60U. This system configuration is shown in Fig.I.1.2-1.

1.2.4 Development of JT-60U plasma equilibrium control model

In general, it is necessary to have a precise model for design and/or optimize a control system. We have developed a plasma equilibrium control model for JT-60, which shows that it can accurately reproduce the time evolution of plasma vertical and horizontal positions on the computer [1.2-4]. This model has been re-built for JT-60U in a workstation by using MATLAB (a system analysis code, made by the Math Works, Inc.). Simulations using this updated model has shown that the control method includes a cause to deteriorate control performance and to induce large voltage fluctuations in a plasma. Since this cause comes from the error in the analog-to-digital conversions and the quantization process in digital computing, a developed new method was predicted to be effective in the simulations to improve the control performance [1.2-5].

This new method was applied to the JT-60 plasma experiments, and we confirmed the plasma control performances are greatly improved as follows [1.2-6]: (1) Control accuracy improvement: The steady-state deviations from the nominal references are reduced to less than 5 mm for Rp with the half of the old control gain, 2 mm for Zp, and 2 mm for Xp with an improved gain. In the Rp-tracking test with the 10-Hz oscillation with 3-cm amplitude, Rp is well controlled by the new algorithm, while the overshooting is observed under the old control algorithm. In the step response, the error of control is less than 10 kA for Ip, and less than 1 cm for Rp, Zp, or Xp. (2) Fluctuation suppression: No irregular fluctuation of the position parameters is observed under the control of the new algorithm. Voltage fluctuation observed in the period under the old control is greatly suppressed by the new algorithm. The reduced amount of peak-to-peak voltage are : 1600 V->300 V (Vertical field coil), 32 V-> 16 V (Divertor coil). In addition, the fluctuation of one-turn voltage difference between inboard and outboard is completely suppressed to 1/10 (3V -> 0.3 V).

1.2.5 Development of the JT-60 new control systems

Since requirements of modification for advanced plasma control and efficient sequential control increase, two control systems began to be developed. Concerning a new plasma control system, we chose an Alpha-288 VME board (made by DEC. Ltd.) for a main processors, and built a VME-bus system together with the I/O boards and a reflective memory module as shown in Fig. I.1.2-2. This system is expected to execute the real-time program approximately 300 times faster than the old mini-computer (1 MIPS), and its performance test is being conducted aiming at installation to the actual system by the second quarter of 1998.

Concerning a new discharge sequential control system, we performed system design of the hardware configuration. This system is composed of three workstations (WS's) with network ports, and each of them has its particular role to supervise the JT-60 subsystems. The roles of the

workstations are as follows: SQ-WS is a master for the sequential control of all the subsystems. This WS sends the all command messages and receives the replies. DC-WS is a master for discharge condition files, and distributes the appropriate condition to the corresponding subsystem, after compiling procedures. RD-WS is a master for result data acquisition. This receives result data from all subsystems, and builds an intermediate file before transferring it to the JT-60 database production server. The new system will be expected to come into operation in 1998.

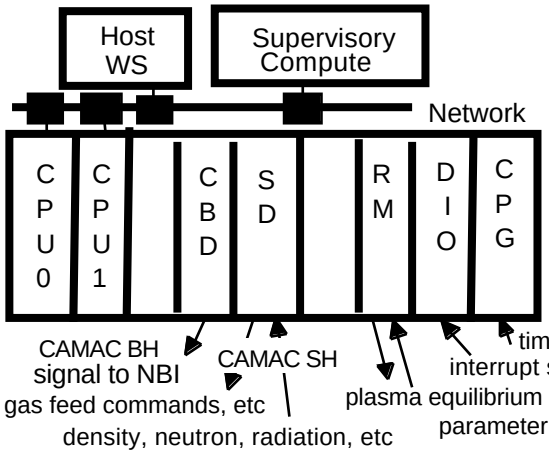

Symbol	Type	Function /Manufacturer
CPU0,1	AXPvme280	DEC 21066A,288MHz,64MB /DEC
CBD	CBD8210	CAMAC Branch Driver / CES
SD	VSHD2992	CAMAC Serial Driver / HYTEC
RM	VMIVME5576	Reflective Memory (256kB) / VMIC
DIO	DSP8230	Digital Input (32 ch) / MTT
CPG	CPG241	Clock Pulse Generator / MTT
WS	Alpha WS 255	UNIX-WS alpha 255MHz / DEC

BH: Branch Highway SH: Serial Highway

Fig.I.1.2-2 Configuration of the plasma real-time control system.

References

[1.2-1] K. Kurihara and Y. Kawamata, "Development of a precise long-time digital integrator for magnetic measurements in a tokamak", in Proceedings of 19th Symposium on Fusion Technology, Lisbon (Portugal, 1996)

[1.2-2] K. Kurihara, Fusion Technol. 22 p.334 (1992).

[1.2-3] H. Adachi, Y. Kawamata, K. Kurihara, "DSP application to fast parallel processing in JT-60U plasma shape real-time visualization," in Proceedings of Symposium on Scientific Research Technologies, Tokyo (1996) (in Japanese).

[1.2-4] K. Kurihara, Fusion Engineering and Design. 19 (1992) 235-257.

[1.2-5] M. Yoshida and K. Kurihara, "The Influence of the Analog-to-Digital Conversion Error on the JT-60 Plasma Position/Shape Feedback Control System," JAERI-Tech 95-053 (1995) (in Japanese).

[1.2-6] K. Kurihara and JT-60 Control Group, JAERI-Review 97-047 (1997).

1.3 Power Supply

1.3.1 Operation and maintenance of the JT-60 power supplies

The JT-60 power supplies were operated on schedule without any serious problems throughout this fiscal year, though thirteen years have passed since they were completed. In November and December 1996 and March 1997, annual maintenance of the power supplies were performed according to the regulations for electric equipment in Naka Fusion Research Establishment. In particular, detailed inspections of two motor-generators for the toroidal field coil power supply (TFPS) and the poloidal field coil power supply (PFPS) were conducted without removing their rotors. The total operation time of the TFPS motor-generator amounts to 13,476 hrs and that of the PFPS motor-generator 13,793 hrs. In the TFPS motor-generator, two oil-pumps

for lifting the thrust bearings up were renewed. A half of guide bearings in the middle stage were replaced by new ones according to the results of liquid penetrant tests (PTs). On the other hand, some mechanical parts of the liquid rheostat (LRH) were renewed and all of the guide bearings in the lower stage were replaced by new ones in the PFPS motor-generator.

1.3.2 Modification of the PFPS for high triangularity operation

Since significant improvements of the plasma performance have been observed in the high triangularity divertor operation with plasma current up to 2 MA in JT-60 [1.3-1], combination of the poloidal field coils and the converters in the PFPS was rearranged for the high triangularity operation (d £ 0.4) with higher plasma current up to about 3 MA. A new connection bus bar switch for changing the operation modes of the "high triangularity", "standard/high elongation" was introduced. The high triangularity operation after the modification is scheduled in June 1997.

Poloidal Field Coil \ Configuration		Standard & High Elongation	High Triangu-larity
Ohmic Heating Coil		PSF + (PSEX)	PSF
Vertical Field Coil	VR-Coil	PSV	PSV
	VT-Coil		(PSQ)
Horizontal Field Coil		(PSQ)	(PSEX) + (PSH)
Divertor Coil		PSM	PSM
Disruption Control Winding		(PSH)	no use

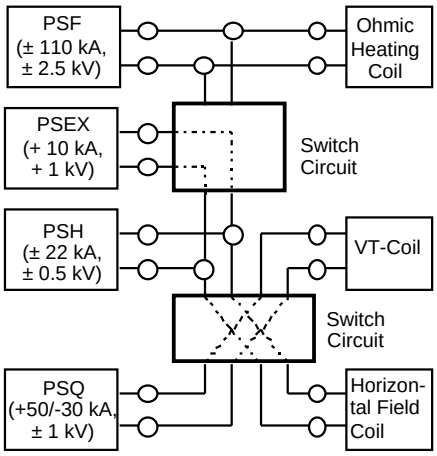

Fig.I.1.3-1 Combination of the poloidal field coils and the PFPS converters for the divertor configurations of "standard", "high elongation" and "high triangularity".

1.3.3 Development of a current-driven PWM converter with high power-factor

As a basic technology development, we have continued to develop a current-driven PWM converter for a superconducting coil power supply, because the semiconductor performance for power applications has been drastically increased up in recent years to be feasible for next generation tokamaks. Since the PWM converter is able to operate with a power factor of unity, the power distortion to commercial transmission lines caused by reactive power fluctuations can be decreased in comparison with conventional thyristor converters. Hence, a PWM converter using IBGTs was developed and tested to clarify its possible technical issues. The output ratings of the designed converter are about 250V and 500A, and the switching frequency is about 1KHz. Results from preliminary tests shows that the pulse modulation method has to be improved to produce zero voltage output with a large current for applying super conducting coils.

References

[1.3-1]Y. Kamada and et al., in Proc. of 16th Int. Conf. on Plasma Physics and Controoled Nuclear Fusion Research, IAEA-

CN-64/A1-6, Montréal, Canada(1196).

1.4 Neutral Beam Injection System

1.4.1 Positive-ion based NBI system

The beam of 40 MW at an energy of around 90 keV, that is the world highest deuterium neutral beam power, has been injected successfully by the simultaneous injection of 14 beamline units. This achievement has been produced through the pursuit of the optimum conditions for the beam acceleration based on the improvement of the accelerator for the ion source. As the result of this injection, the JT-60 has been able to expand the plasma experimental area with a higher power NBI heating.

1.4.2 Negative-ion based NBI system

The beam injection experiment for the negative-ion based NBI system (N-NBI) has been continued, augmenting the beam power gradually, ever since the beam into the plasma by the N-NBI had been injected successfully for the first time in the world in March 1996. The deuterium neutral beam of 2.5 MW at an energy of 350 keV has been injected with two ion sources in September 1996. As this result, it was confirmed that the characteristics of the NBI current drive and plasma heating with a high neutral energy beam have agreed with a theoretical estimation.

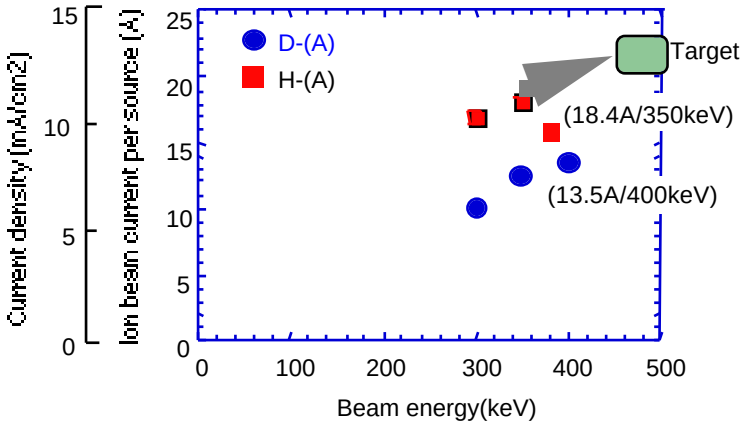

Fig. 3.1.3.9 Progress of negative ion beams in the N-NBI for JT-60

After the partial remodeling for the ion source and the power supply, the hydrogen neutral beam of 3.2 MW at 350 keV has been injected with one ion source in February 1997. And the negative-ion beam power per one ion source has reached 400 keV, 13.5 A with deuterium and 350 keV, 18.4 A with hydrogen, that is the world highest negative-ion beam. They are shown in Fig.I.1.4-1.

The current drive and plasma core heating experiments with the N-NBI will be progressed strongly in JT-60, aiming at a rated injection power of 10 MW, for the establishment of the technical and physical bases of the ITER construction.

1.5 Radio-frequency System

1.5.1 LHRF system

The lower hybrid range of frequencies (LHRF) system has contributed to successful experiments on the reversed magnetic shear mode [1.5-1] and assist for start up of plasma current [1.5-2] mainly in FY 1996. Total shot numbers of the discharge supported by LH injection for A,

B and C units are 369, 379 and 315, respectively. The maximum generated power of 8-klystrons for A, B and C units are 3.4, 3.0 and 2.6 MW, respectively . The main troubles in this FY were 1) degradation of klystrons due to reduced standoff capability around electron gun, and 2) malfunction in the crowbar circuit of C unit triggered by electric noises from the negative ion based NBI system.

An RF breakdown in the antenna mouth could cause serious damages of the antenna. In order to avoid heavy breakdown in the main vacuum part of the antenna, an additional arc detector was equipped in the antenna system as shown in Fig. I. 1. 5-1. When arc lights detected, RF injection is immediately shut down during 100 msec and then is restarted by the protection system. This arc detector works only during RF injection to distinguish the arc from relative strong stray lights at the plasma initiation of the discharge. The arc detector is a key device for efficient antenna-conditioning without terrible breakdown.

In addition, as an efficient conditioning technique of the antenna, RF injection pulse was modulated with intermittent short pulses, for example, pulse length of 20 msec and duty of 50 %. This pulse-modulated injection could lead to stable power up without hard breakdown, while with small breakdown necessary for progress of the conditioning. Therefore , the damage of the antenna is reduced, and plasma shot number required decreases. For the current drive

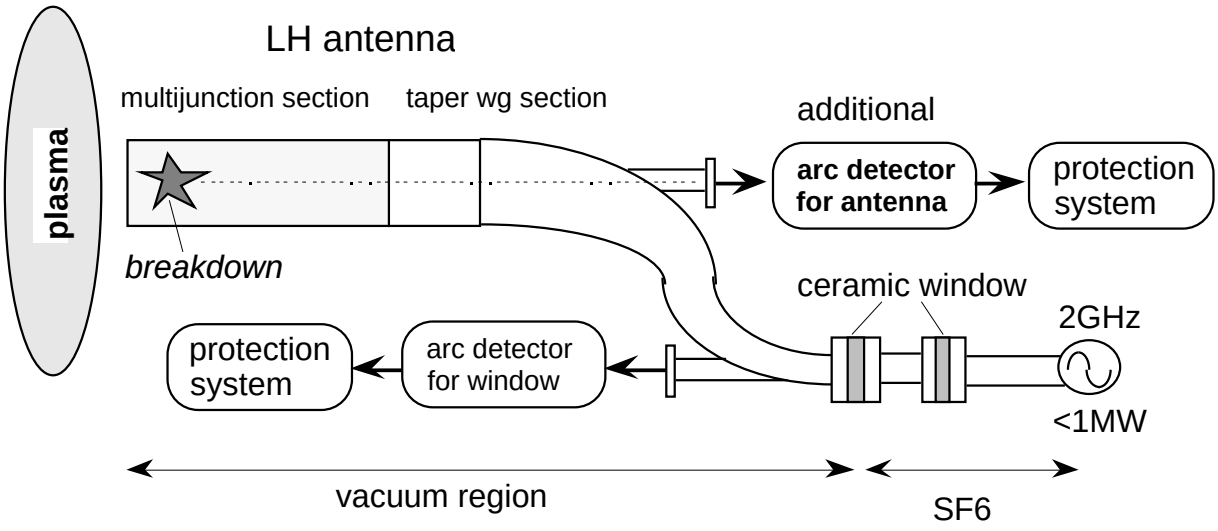

Fig. I.1.5-1 Arc detector system for antenna and RF window

experiments using pulse-modulated injection, the current drive efficiency did not degrade under the same averaged input power. The hard X-ray profile showed a little bit wider, namely broad current profile, in pulse-modulated injection compared with that of no modulation.

1.5.2 ICRF system

The ion cyclotron range of frequencies (ICRF) system was operated well at 102 MHz in FY 1996. The frequency of the system was changed to 102 MHz from 116 MHz in December 1995,

in order to keep up central plasma heating with the low toroidal magnetic field (B_T) operation. The resonant B_T of the second harmonics of hydrogen was reduced from 3.8 T to 3.34 T. From January 1996, RF power at 102 MHz had been injected to the plasma occasionally. Impedance matching between the antenna and the transmission line using the stub tuners and the high power phase shifters, adjustment of the phase control, and the antenna conditioning were taken place. About 80 shots were devoted to impedance matching and antenna aging after the frequency change. Following the antenna aging, the coupled power reached 4.3 MW (short pulse) in 80 shots and 4.6 MW for 1 sec at last in November 1996. The maximum stand-off voltage in the antenna was ~ 34 kV and is close to the maximum voltage achieved at 116 MHz. It means that low coupling resistance limited the coupled power.

At 102 MHz, the coupling resistance of the antenna, R_C, was 60 - 70% of that at 116 MHz [1.5-3]. Figure I.1.5-2 shows the R_C versus the gap between the separatrix and the first wall of the vacuum vessel on equatorial plane. The Faraday shield of the ICRF antenna is ~ 3 cm behind the first wall surface. The stand-off voltage in the antenna versus the coupled power P_{IC} at 102 MHz and 116 MHz is shown in Fig. I.1.5-3. It is clear that the P_{IC} at 102 MHz was limited by the antenna voltage stand-off.. In contrast with at 102 MHz, P_{IC} at 116 MHz was limited mainly by the generator capability [1.5-4]. Reduction of R_C results from RF characteristics of the antenna which was designed to obtain best coupling at ~ 120 MHz. For the closed divertor plasma expected in the operation in 1997, a little larger antenna-separatrix gap and lower SOL density due to the baffle plate are foreseen, and then lower R_C is expected. Improvement of antenna voltage stand-off of the coupling system is effective to couple higher power.

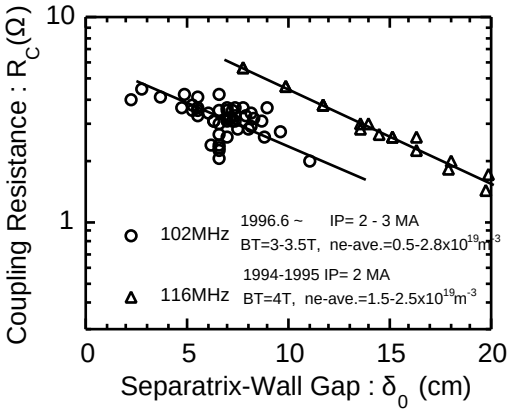

Fig. I.1.5-2 Coupling resistance at 116 and 102 MHz voltage

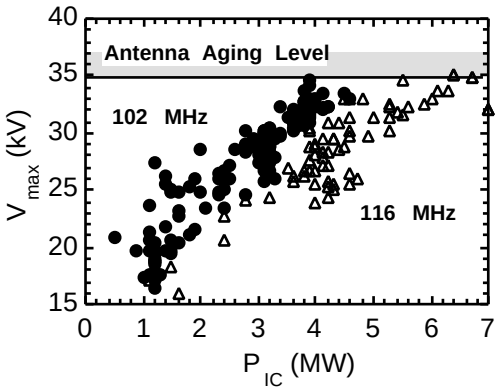

Fig. I.1.5-3 Coupled power limited by the antenna stand-off at 102 MHz.

To increase the stand-off voltage, short plunger and outer conductor of the stub tuner were newly designed and fabricated. The new plunger is a conservative mechanical contact type as a substitution of the former choke plunger, which acts as a equivalent short circuit without

mechanical contact. The choke plunger had an advantage in capability of quick movement during high power RF pulse. However the choke plunger requires precision in narrow gaps in its structure to keep high voltage stand-off capability. When the uniformity of the gap is lost after lots of operations for many years, the arcing tends to occur in high voltage operation and damages the structure. Importance of quick movement of the plunger during the discharge shot had become lower because frequency feedback control works well to keep good impedance matching.

For the new contact type plunger, "multilam band" is used as a contact element, as well as the high power phase shifter. Reliability of the contact element is confirmed in a 10 thousand strokes' endurance test of the high power phase shifter. The new short plunger will be installed in the stub tuner in April 1997.

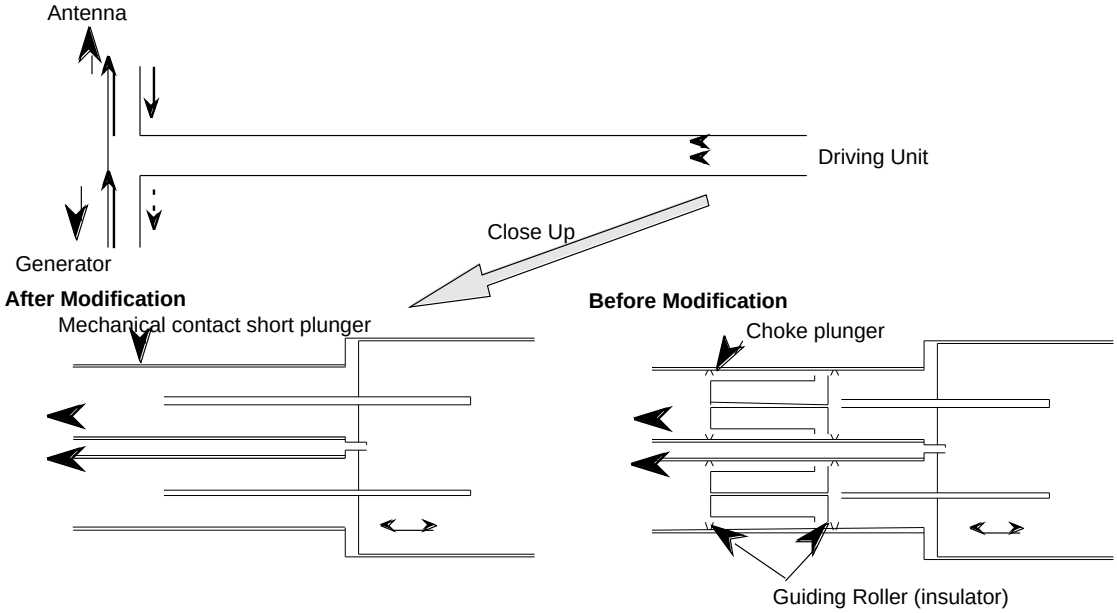

Fig. I.1.5-4 Modification of the Stub Tuner

Reference

[1.5-1] S. Ide, M. Seki, et al., "Sustainment and Modification of Reversed Magnetic Shear by LHCD on JT-60U", Plasma Physics and Controlled Fusion 38 (1996) 1645-1652.

[1.5-2] R. Yoshino, M. Seki, "Low electric field (0.08 Vm-1) plasma-current start-up in JT-60U", Plasma Physics and Controlled Fusion 39 (1997) 205-222.

[1.5-3] S. Moriyama, et al., "ICRF Coupling at 102 MHz", Review of JT-60U Experimental Results from January to November 1996, Section 5.4, JAERI-Research, 1997.

[1.5-4] S. Moriyama, et al., "ICRF Coupling Study and Technology Development for JT-60U", Proc. US-Japan workshop for RF technology, Florida, Dec. 1995.

1.6 Diagnostic System

During the reconstruction phase of the divertor, electrostatic probes, a reciprocating probe, mm-wave interferometers, multichannel borometers, a visible fiber array, ion gauges and Penning gauges were newly installed for the detailed study of the divertor plasmas. Significant progress was also made in the diagnostic system as described in the following sections.

1.6.1 Automatic analysis of sawtooth inversion radius with adaptive neural network [1.6-1]

A neural network algorithm was applied to the electron cyclotron emission (ECE) data of JT-60U plasma, and sawtooth inversion radii are automatically acquired to obtain information concerning current profiles. To detect the time of sawtooth collapse, a method of adaptive signal prediction by a three-layered perceptron is applied to the time series of ECE data which were obtained by a grating polychromator system. The collapse time is determined from the time when the prediction error is maximized in magnitude. This work was performed by a collaboration with Toyama Kenritsu University.

1.6.2 Elimination of non-thermal emission from FTS interferogram during ELM[1.6-2]

A Fourier-transform spectrometer system (FTS) is used for the measurement of time evolution of electron temperature profile. In the ELMy H-mode phase, however, electron temperature measurement by FTS becomes difficult because the interferogram suffers from intense non-thermal emission from plasma which relates to ELM. In order to remove and reconstruct the interferogram, a high-pass filter and smoothing method is applied. The electron temperature deduced by Fourier-transforming the reconstructed interferogram showed a good agreement with the result of a relatively calibrated grating polychromator system.

1.6.3 Determination of radial position in the measurement of electron temperature profiles from ECE [1.6-3]

The effects of relativistic frequency down-shift and optical thickness at the medium electron temperatures are important to determine the radial position of the electron temperature profile from the electron cyclotron emission. Exclusion of the effects in the determination results in a pseudo radial displacement (Δr) of the obtained electron temperature profile. The displacement depends on only three parameters (electron temperature, T_e, optical depth, τ, and major radius, R). In order to evaluate the radial position correctly for any tokamak, a scaling of the displacement is found as Δr (m)= 0.0009 R(m) T_e(keV) (1+ 40/(5τ)). This scaling is applicable for $\tau > 5$ where the error is less than 0.5% of the major radius.

1.6.4 Upgrade of MSE diagnostics

A new polarimeter with nine viewing points for the motional Stark effect (MSE)

spectroscopy was installed in December, 1995 in addition to the old one [1.6-4]. By using old and new polarimeters, we can measure the region of R = 3.04-4.29 m with 14 chords, which almost covers from the axis to the surface for a standard configuration. To reduce the error by background light, multi-layer dielectric mirrors are used in the new spectrometer. The aluminum-coated mirrors in the old polarimeter have also been changed to multi-layer dielectric mirrors. The whole MSE system had been operated routinely in 1996 and safety-factor profiles were obtained in various types of discharges.

1.6.5 Optical fiber array viewing divertor region for 2-dimensional spectroscopic measurement

A 32-channel optical fiber array system viewing the divertor region from the side was installed to measure poloidal emission profiles of hydrogen isotopes and impurities. This array system guides the visible light emitted in the divertor region to a spectrometer composed of filter optics. The emission profiles of five different spectral lines are measured simultaneously by this spectrometer with a 32-ch photomultiplier array at a fast sampling rate of 160 μs and with photodiode arrays at a slow sampling rate of 2.8 ms. The poloidal contours of spectral emissions in the divertor region are constructed by analyzing both emission profiles from this system and from a existing 60-channel optical fiber array system viewing from the top.

1.6.6 Fast sampling charge exchange recombination spectroscopy [1.6-5]

A Charge exchange recombination spectroscopy (CXRS) system with a three interference filter assembly and photomultipliers has been developed for the faster measurements of ion temperatures (*Ti*) and toroidal rotation velocities (*Vt*). Each filter has a 0.2 - 1 nm bandwidth (FWHM), and the three filters have a slightly different peak wavelength to its selected CXR line, depending on the *Ti* and *Vt* at the measuring position. 12 assemblies viewing on and off the neutral beam line were installed for the space-resolved *Ti*, *Vt* and the background measurements. The maximum sampling rate of this system is 160 μs. This is faster than 16.7 ms of the existing CXRS system composed of spectrometers and CCD cameras.

1.6.7 Neutron fluctuation measurement system [1.6-6]

In JT-60U, neutron emission monitors with the time resolution of 1ms and 14 MeV - neutron detectors with the time resolution of 10 ms have been used from the beginning of the DD discharges. In this fiscal year, the neutron detector with a fast time resolution of 40 μs and a spatial resolution of 15 cm was installed in order to study the correlation between the MHD behaviors (such as sawtooth activities and fishbone instability) and the neutron emissions. The detector, which is composed of a plastic scintillator (NE102A) and a photomultiplier, is operated in the current mode to get a fast response. The detector is mounted approximately 2 m away from the surface of the vacuum vessel near the mid plane.

References
[1.6-1] Isei N., Ooi Y., Iwama N., et al., to be submitted to Jounal of Plasma and Fusion Research.
[1.6-2] Isayama A., Isei N., Ishida S., et al., JAERI-Research 97-047, 138 (1997).
[1.6-3] Sato M., Isei N., Isayama A., et al., (Proc. International Conference on Plasma Physics, Nagoya, Japan 1996) Vol. 2, p.1438.
[1.6-4] Fujita T., Kubo H. and Oikawa T., JAERI-Research 97-047, 143 (1997).
[1.6-5] Koog J.S., Sakasai A., JAERI-Research 97-047, 146 (1997).
[1.6-6] Morioka A., Nishitani T., Kondoh T., et al., JAERI-Research 97-047, 148 (1997).

1.7 Data Analysis System

1.7.1 FAME system

The FAME (Fast Analyzer for Magnetohydrodynamic(MHD) Equilibrium) system has been developed in 1993 to provide about 130 MHD equilibria in time series which are enough for the non-stationary analysis of the experimental data of JT-60U within a shot interval. The FAME system have stored all the equilibrium data in JT-60U from 1993. In FY1996, the efforts of utility development and update have been concentrated on more effective use of the FAME system. An equilibrium animating system has been developed on a workstation arranged in the central control room. The system can provide animations of MHD equilibrium analyzed by the FAME. In order to display typical equilibrium data such as an ellipticity, an internal inductance, and so on as functions of time with other experimental data, the DAISY (DAta Illustration SYstem) and the software of FAME system are improved.

The new system, FAME-II, with a high processing speed utilizing IBM RS/6000 SP is being introduced, succeeding the former FAME system. The FAME-II system is a MIMD type small scaled parallel computers with 7 microprocessors and the maximum theoretical speed is 3.42 GFLOPS. For the software system of FAME-II, MHD equilibrium analysis code SELENE and its input data production code FBI are tuned up taking the parallel processing into consideration as well as the former FAME system. Consequently, the computational performance of the FAME-II system for special use of JT-60U equilibrium analyses becomes more than 3 times faster than the existing FAME system. The new system also has the file server system with the large capacity of the mass data storage of 50 GB, which can afford to store all the equilibrium data in JT-60U for coming 3 years.

1.7.2 Data Link System and Video Conference System

The effectiveness of the remote participation in JT-60 experiments from PPPL was successfully demonstrated during QDT >1 campaign from the end of October to the beginning of November, by utilizing the Data Link System and the video conferencing systems. Participants from both JAERI and PPPL jointly analyzed and discussed the JT-60 data and recognized achievement of a high fusion performance in JT-60 reversed shear discharges. This success is

envisaged to be a new model of the international collaboration via computer and communication networks for the twenty-first century.

In July '96, a remote diagnostics operation and a remote data analysis were simultaneously tested. A neutron diagnostic system on the JT-60 has been successfully operated from Los Alamos National Laboratory (LANL) via the JAERI- DOE leased, overseas line. Remote analysis of JT-60 data from PPPL was done by using the Data Link System and the video conferencing systems for the discussion between JAERI and PPPL.

In October '96, the Data Link System was completed for exchanging experimental data of JT-60 through the Data Link. Selected data among approximately 2100 typical JT-60 shots were transferred to this system for the use under the regulation of remote access under the Three Large Tokamak Agreement. A new database of detailed experimental data with the amount of 6MB per diagnostic for each shot were also prepared.

The Data Link System provided data analysis tools; a first magnetic boundary identification code (FBI), a MHD equilibrium analysis code (SELENE), and a plasma profile monitoring tool (SLICE).

A multi-point bridge system was introduced for ISDN based video-conferencing capabilities to enable multi-point connections. The JT-60 control room is now connected to PPPL and LANL via the video conference systems using ISDN lines.

1.7.3 Computer System and Database

The main frame of computer system have been replaced from the MSP operating system on FACOM M-780 (FEP) to the UNIX operating system on workstations due to the plan organized by the Center for Promotion of Computational Science and Engineering. According to the plan, all plasma analysis codes, utility codes, and many databases have been transplanted to the new system. Especially, computer graphic programs and data handling programs have been almost newly developed for the UNIX system. The preparation of the transplantation had been started from FY1994 and carefully carried out. The new UNIX system have enabled to realize a distributed processing system and augment the data processing capacity by about 10 times.

The database related software was also largely changed. The database structure was redesigned to a more flexible one and database managing programs, NDBS, were converted from the original one on FEP. A network data transfer program, IFDB, was also ported from the original ISP-to-FEP version. After the completion of CO2 interferometer, YAG Thomson scattering system and scintillating fiber neutron detectors, their data were added to JT-60 experimental database. Plasma equilibrium data calculated by FAME system were also added.

Some subsystems and programs of JT-60 data processing system were improved during FY1996 to replace aged mini-computers and meet the demands of plasma diagnostic systems. Since January 1996 a workstation-based prototype CICU system had been tested in detail on

behalf of one of present CICU systems based on mini-computers. After the improvement of hardware and software components, the final design of new CICU systems was completed. New CICU systems consist of VME modules with CAMAC serial highway drivers. They have been under a practical test for the complete replacement of CICU systems.

A new mass data acquisition system, FDS, was developed. It uses a UNIX workstation and a VME-based opto-electric conversion module with memory. It would be used as a successor to a present minicomputer-based TMDS system. New programs to calculate physics data from TMDS raw data were developed for some diagnostic systems and the results were stored as a new database in the JT-60 file server or the newly introduced TMDS server.

Reference

[1.7-1] Hamamatsu K., Matsuda T., Nishitani T., et al.," Remote Laboratory in Fusion Experiments, Present Status and Progress", J. Plasma Fusion Res., **73**, 385 (1997) (in Japanese)

[1.7-2] Aoyagi T., " Data Processing System for JT-60", J. Plasma Fusion Res., **72**, 1370 (1996) (in Japanese)

2. Experimental Results and Analysis

2.1 Reversed Shear Experiments

2.1.1 Achievement of high fusion performance [2.1-1, 2]

Significant improvement in fusion performance has been achieved in thermonuclear fusion regime with 16 MW of deuterium-neutral beam injection into reversed shear discharges at 2.8 MA of plasma current. The core plasma energy is efficiently confined due to the internal transport barrier formed for both ions and electrons at ~70% of the plasma minor radius near the boundary of the negative shear region.

In the best shot the plasma stored energy increased up to the JT-60U record value of 10.9 MJ with a high DD neutron emission rate of 4.5×10^{16} /s. Plasmas that could have been produced in an assumed D-T (deuterium-tritium) fuel are simulated by using the TOPICS code and the TRANSP code simply considering the full D beams with the experimental beam energy into a plasma of 50:50 D-T mixture. Good agreements are obtained with confidence among these analyses for D-D analysis and D-T simulation. The projected fusion power is equivalent to 10.7 MW with 83% from thermonuclear reactions. This large fraction of thermonuclear reactions should be emphasized in contrast to the other high performance regimes such as TFTR supershot, JET hot ion H mode and JT-60U high β_p H mode, in which substantial fraction of fusion power came from beam-thermal reactions. A simple ratio of the fusion power to the actual beam absorption power, P_{DT}/P_{abs} would be 0.68. For transient plasmas, the fusion amplification factor can be defined from the effective heating power that can be estimated by subtracting the dW/dt term (the loss power from the plasma) from P_{abs} [2.1-3]. Following this definition, the equivalent fusion amplification factor Q_{DT}^{eq} reached 1.05 with a high fusion triple product of $n_D(0)\tau_E T_i(0) = 7.8 \times 10^{20}$ m^3•s•keV. The remarkable progress in fusion performance can be attributed to the stable increase in plasma current with a wide reversed shear region up to 70-80% of plasma minor radius (see Fig.I,2,1-1) and a well optimized control of the beam deposition profile during the current ramp-up. The high performance reversed shear plasmas, which had an L-mode edge, terminated into a disruptive beta collapse when q_{min} decreased to ~ 2. Pressure profile broadening with an H-mode edge would improve the stability and lead to a quasi-steady-state operation as observed in the high β_p H mode [2.1-4].

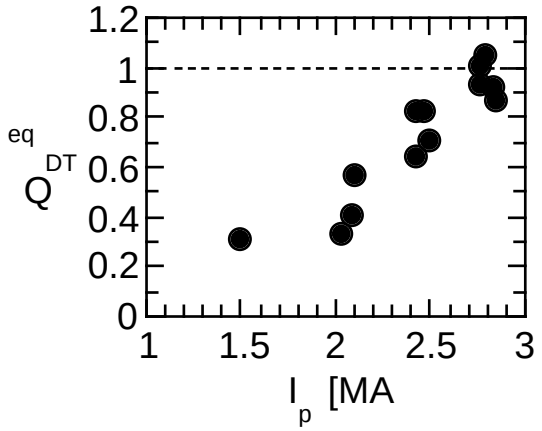

Fig. I.2.1-1. The calculated Q_{DT}^{eq} as a function of plasma current, Ip, for reversed shear discharges. The fusion performance has been improved with the incease in Ip.

2.1.2 Internal transport barrier and confinement [2.1-2, 5, 6, 7]

Steep gradients in profiles for electron density, electron temperature and ion temperature, which indicate the formation of Internal Transport Barrier (ITB), are observed in JT-60U reversed shear plasmas. Significant reduction of thermal transport are obtained both for ions and for electrons [2.1-8]. The steep gradient zones have a radial extent of ~20% of plasma minor radius and are located inside the radius of q_{min}. To obtain high performance plasmas, it was essential to form a q profile with a large radius of q_{min} (up to 80% of plasma minor radius) in a low q regime (q_{min} ~ 2). The formation of ITB in an early phase and the control of pressure and current profiles during the current ramp-up with keeping the ITB were key techniques to obtain a large radius of q_{min} in a low q_{min} regime [2.1-6]. The ITB was formed by on-axis beam heating into a low density target plasma with reversed shear that was formed by current ramp-up without beam heating. The foot (outer edge) of ITB was formed at ~0.45a at first and moved outward up to ~0.8a while the position of q_{min} also moved outward from ~0.65a to ~0.8a. The foot of ITB was located at or inside the radius of q_{min}, which was observed in many discharges with the radius of q_{min} ranged between 0.5a and 0.8a. The energy confinement time increased with the increase in the radius of ITB and with the decrease in q_{min} for a fixed toroidal field. High H factors, $\tau_E/\tau_E^{ITER89P}$, up to 3.3 were obtained with an L-mode edge. The effective one-fluid thermal diffusivity in the ITB was less than the value predicted by Chang-Hinton's neoclassical theory. The reversed shear plasmas are characterized by the achievement of high confinement with relatively low beam power (P_{abs} ~12.5 MW), while high confinement is obtained in high power regime (P_{abs} ~25 MW) for the high β_p H mode [2-1.5]. The values of H/q_{95} and β_t increased with the increase in the plasma current (or the decrease in q_{95}), and the highest performance was achieved at q_{95} = 3 (2.8 MA). The performance was limited by disruptive beta collapses with β_N ~ 2 at q_{min} ~ 2.

2.1.3 MHD activities and stability [2.1-7, 9, 10]

Various MHD fluctuations including resistive modes and ideal modes were observed in JT-60U reversed shear discharges.

Resistive modes, which were observed continuously, can be classified by their localization in the minor radius; near ρ_{ITB}, at distinctly inside or outside of ρ_{ITB}, and near the plasma surface. Here, ρ_{ITB} is the normalized radius at the steep pressure gradient generated by the ITB. Resistive modes localized near ρ_{ITB} were observed, when the pressure gradient and β were large enough and q_{min} was between integer values. Fluctuations with and without in-out asymmetry were observed in electron temperatures. Resistive modes without in-out asymmetry seem to be the double tearing mode while resistive modes localized near ρ_{ITB} with in-out asymmetry are not identified yet. Most of reversed shear discharges with an L-mode edge were terminated with a hard collapse which resulted in the disruption. The upper limit of the achieved β_N in reversed shear

discharges lies in the same region with that in high β_p discharges. On the other hand, hard collapses in reversed shear discharges often occurred even in the quite low β_N region. The hard collapses in the low β_N region sometimes occurred at $q_{min} \sim 4$ or $q_{min} \sim 3$ with the growth time of the ideal MHD instabilities. Some of low β_N collapses seemed to be associated with surface modes such as external kink modes, because β_N collapses sometimes occurred when the NB injection power was reduced and the surface q was close to integer values. We also observed a growth of the rotating mode near the plasma surface and the mode locking for hard collapses. Before hard collapses at $q_{min} \sim 2$, precursor oscillations in electron temperatures were observed to be localized in the ITB region. The amplitude of the precursor oscillations increased with the growth time longer than 1.5 ms, which is in the growth time range of resistive MHD instabilities. The collapse, which followed these resistive modes, explosively grew from the ITB region with a very fast growth time of the order of ~ 10 μs. Ideal MHD stability analysis showed that the experimental beta limit ($\beta_N \sim 2$) at $q_{min} \sim 2$ is close to the theoretical one for the ideal low n (n=1) kink modes [2.1-11].

2.1.4 Formation, control and sustainment of reversed shear by LHCD [2.1-12, 13]

By using lower hybrid wave (LHW) current drive (LHCD), it has been experimentally demonstrated that reversed magnetic shear can be maintained and controlled [2.1-13]. Formation of a reversed magnetic shear configuration by an LHW injection alone was successfully demonstrated [2.1-12]. Strongly reversed magnetic shear, which is even stronger than one formed by a normal scenario (NBI heating at current ramp-up), with large area of shear reversal was formed by an LHW injection alone. Furthermore, intense gradient was found in the electron temperature profile, which suggested the confinement improvement. Moreover, the attainable β_N in this discharge was comparable to that of normal reversed shear discharge.

References

[2.1-1] Ishida S., Fujita T., Asakura N., et al., submitted to Phys. Rev. Lett. (1997).
[2.1-2] Koide Y. and the JT-60 Team, Phys. Plasmas **4**, 1623 (1997).
[2.1-3] JET Team, Nucl. Fusion **32**, 187 (1992).
[2.1-4] Mori M., Ishida S., Ando T., et al., Nucl. Fusion **34**, 1045 (1994).
[2.1-5] Fujita T., Ide S., Kimura H., et al., to be published in Proc. 16th IAEA Fusion Energy Conf., Montréal, 1996, IAEA-CN-64/A1-4.
[2.1-6] Fujita T., Hatae T., Oikawa T., et al., submitted to Nucl. Fusion (1997).
[2.1-7] Neyatani Y. and the JT-60 Team, Plasma Phys. Controlled Fusion **38**, A181 (1996).
[2.1-8] Fujita T., Ide S., Shirai H., et al., Phys. Rev. Lett. **78**, 2377 (1997).
[2.1-9] Takeji S., Fujita T., Ozeki T., et al., JAERI-Research 97-047, 10 (1997).
[2.1-10] Ishida S., Takeji S., Isayama A., et al., to be published in Controlled Fusion and Plasma Physics (Proc. 24th Eur. Conf. Berchtesgaden, 1997).
[2.1-11] Ozeki T., Azumi M., Ishii Y., et al., Plasma Phys. Control. Fusion **39**, A371 (1997).
[2.1-12] Ide S., Naito O., Fujita T., et al., to be published in Proc. 16th IAEA Fusion Energy Conf., Montréal, 1996, IAEA-CN-64/E-3
[2.1-13] Ide S., Fujita T., Naito O., et al., Plasma Phys. Controlled Fusion, **38**, 1645 (1996).

2.2 High-β_p H-mode and High Triangularity Discharges

2.2.1 High β_p H-mode confinement at high current with high power neutral beam injection

The high-β_p H-mode discharges, which may bring out more higher fusion triple product, are configured to achieve a peaked beam deposition profile with a large aspect ratio A~4.3 and a low triangularity δ~0.05. It is essential for achieving the high-β_p H-mode confinement to create a sawtooth-free target plasma with a central q slightly above unity by injecting the main beams before the sawtooth onset, which would have produced a weak central magnetic shear configuration. The new technical advancements also contributed to high-β_p H-mode JT-60U experiments in 1996 are as follows:

1) fast current ramp-up operation allowing the main beams to be injected in the current flat top phase at high currents up to 2.7 MA

2) intense beam power of up to 41 MW at 90-95 keV.

The highest fusion triple product $n_D(0)\tau_E T_i(0)$ was transiently achieved with high additional heating power injection of 37 MW at the maximum and Z_{eff}~2.2 at q_{95}=2.9 during an ELM-free high-β_p H-mode, where $n_D(0)\tau_E T_i(0)$ reached ~1.5 x $10^{21}m^{-3}$•s•keV with the central ion temperature T_i=45±5 keV, the stored energy W_{dia}=8.6 MJ, and the neutron yield S_n=5.2 x 10^{16} /s at the maximum. The high performance high-βp H-mode plasma was also sustained at q_{95}=3.0 with successive ELMs.

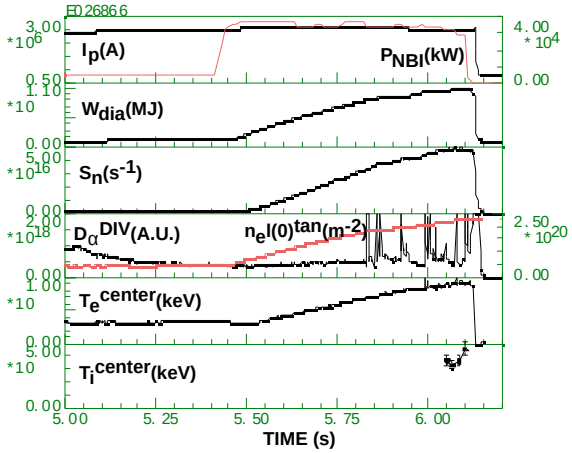

Fig.I.2.2-1 Discharge waveforms of a record shot to show the highest stored energy in high-β_p H-mode.

As shown in Fig.I.2.2-1, W_{dia} and S_n reaches 9.3 MJ and 4.9 x 10^{16} /s and $n_D(0)\tau_E T_i(0)$~5.1 x $10^{20}m^{-3}$•s•keV was achieved at peak, respectively. It is found that both W_{dia} and S_n increase with increase of plasma current above 2.2 MA. These experimental evidences showing that the fusion performance is peaked around q_{95}~3 independent of transient, stationary states (dW/dt~0) support the argument that the fusion performance can be maximized around q_{95}~3 where ITER would have achieved self-ignition. In the high-βp mode phase just before the H- mode transition, the presence of internal transport barrier is clearly indicated in the electron density and ion temperature profile at r/a ~ 0.7 while the q profiles measured from motional Stark effect spectroscopy reveals the central q value of ~ 1.4 slightly above unity with a weak central shear [2.2-1].

References

[2.2-1] S.Ishida, Y. Neyatani, Y. Kamada, A. Isayama, T. Fujita et al., in Plasma Physics and Controlled Nuclear Fusion Research 1996 (Proc. 16th Int. Conf. Montreal, Canada 1996),.

2.3 H-mode Study

Impact of the neutral particles on the H-mode transition power threshold has been studied [2.3-1]. The fact that the compiled threshold database from various tokamaks has not yet been successful hitherto in providing a unique and reliable threshold power scaling is mainly ascribed to the ambiguities involved with the size and density dependencies. In particular, the density dependence is regarded as the most crucial but difficult to analyze issue, due to its sensitivities to the wall conditions. Based on the results of deliberate experimental investigations at JT-60U, we have first documented that (1) the edge neutral particle density literally determines the degree to which the threshold power depends on the density, and (2) the density boundary, below which the H-mode transition cannot occur, may also be governed by the edge neutrals. Therefore, information on the edge neutral particles can integrate the different density dependencies observed in various tokamaks, and thereby a firm ground for the size scaling may also be established, which can well be extrapolated to a fusion reactor with an adequate precision.

Dependence of transport properties on the normalized gyro-radius ρ^* has been studied on ELMy H-mode plasmas with high triangularity δ in JT-60U [2.3-2]. The thermal diffusivity χ is expressed as $\chi = (T_e/eB)(\rho^*)^{\mu} F(\beta, \nu^*,...)$, where F is a nondimensional function with β, ν^* etc. Because the ρ^* value of ITER is much smaller than that of large tokamaks, the ρ^* dependence of χ is an important subject to predict the transport properties of ITER plasmas. In ELMy H-mode plasmas with low δ value, the normalized thermal energy confinement time, $\tau_{th}T_e/eB_t$, was found almost independent of ρ^* due to the strong ELM activity occur in the high B_t shot [2.3-3]. The high δ configuration ($\delta = 0.35$) applied here is expected to suppress the ELM activity. A pair of NBI heated ELMy H-mode shots with B_t =1.86 T and 3.08 T are compared. Nondimensional parameters except ρ^* are the same and $T_i/T_e \approx 1$ in $1/3 < a/r < 2/3$ for both shots. It is found that the ρ^* dependence of χ_e is almost the same or somewhat stronger than that in L-mode plasmas, i.e., $\mu \approx 0.5$, while the χ_i becomes almost gyro Bohm type diffusion, i.e., $\mu \approx 1$. The confinement time is almost inversely proportional to $\tau_{th}T_e/eB_t \quad (\rho^*)^{-0.8}$ which is favorable for the future reactor. This results is similar to those obtained in JET and DIII-D.

The relative change of the electron and ion thermal diffusivity, $\delta\chi_e/\chi_e$ and $\delta\chi_i/\chi_i$, and that for the improvement of thermal energy confinement, δTH/TH, at the H-L transition has been studied in JT-60U ICC (Improved Core Confinement) H-mode plasmas with I_p = 1.6~3.5 MA and $B_t \approx 4.0$ T [2.3-4]. Here the change is defined as $\delta\chi = \chi(t_+) - \chi(t_-)$ across the transition at the time t. The improvement factor TH is determined on the basis of the L-mode thermal confinement time scaling. As for $\delta\chi_e/\chi_e$, it is large (0.5~0.6) even for small δTH/TH value (=0.15) and changes very little with the increase of δTH/TH. On the other hand, $\delta\chi_i/\chi_i$ increases with δTH/TH. The improvement of total thermal confinement in H phase is dominated by the reduction of ion heat transport. The relative change of the effective particle diffusivity, δD/D, is independent of δTH/TH.

The width of the edge pedestal Δr has been investigated for ELM-free H-mode plasmas in JT -60U [2.3-5]. The width plays an important role to determine the stability of ELM. Edge pedestals of electron and ion temperature profiles are measured over a wide range of plasma current from 1 MA to 4.5 MA. The results show that Δr is linearly scaled with $\sqrt{\varepsilon}\,\rho_{pi}$ as the prediction in Shaing's theory, where ε is the inverse aspect ratio and ρ_{pi} is the poloidal gyro-radius for thermal ions. The value of Δr is a factor ~4 larger than the theoretical prediction

In order to predict the threshold power for the L-H transition and the energy confinement performance in ITER, databases have been assembled and are being analyzed [2.3-6]. Data from JT-60U and JFT-2M contribute to these ITER database. The ITER Threshold Database includes data from 10 divertor tokamaks. This database gives a scaling of the threshold power of the form $P_{thr} \propto B_t\, n_e^{0.75}\, R^2 \times (n_e R^2)^{\pm 0.25}$, which predicts $P_{thr} \approx 100 \times 2^{0\pm1}$ MW for ITER at $n_e = 5 \times 10^{19}$ m^{-3}. The ITER L-mode Confinement Database has also been assembled from 14 tokamaks, and a scaling of the thermal energy confinement time τ_{th}^{L} in L-mode and ohmic phases has been obtained. With the ITER parameters, τ_{th}^{L} is about 2.3 sec. For ignition in ITER, more than 2.5 times this value will be required. The ITER H-mode Confinement Database has been expanded from the data of 6 tokamaks to the data of 11 tokamaks. A τ_{th} scaling for the ELMy H-mode has been obtained by a standard regression analysis and predicts for ITER a confinement time $\tau_{th} \approx 6 \times (1 \pm 0.3)$ sec. The degradation of τ_{th} with increasing $n_e R^2$ (or decreasing ρ_*) is not found for ELMy H-mode. An offset-linear law scaling with a dimensionally correct form also predicts nearly the same τ_{th} value.

References

[2.3-1] Fukuda T., Sato M., Takizuka T., et al., 16th IAEA Fusion Energy Conference, Montreal, (1996) IAEA-CN-64/AP2-9.

[2.3-2] Shirai H., Takizuka T., Kamada Y., et al., "Nondimensional Transport Study on ELMy H-mode Plasmas in JT-60U", in JAERI-Research 97-047 (1997).

[2.3-3] Takizuka T., Shirai H., Kamada Y., et al., "Nondimensional Transport Experiment in JT-60U", in JAERI-Research 95-075 (1995) 22.

[2.3-4] Shirai.H, Takizuka T., Sato M., et al., "Analyses of Electron and Ion Transport Properties in JT-60U H-mode Plasmas with Improved Core Confinement", proc. 23rd EPS Conf., Kiev, Part I (1996) 339.

[2.3-5] Hatae T., Ishida S., Kamada Y., et al., "Edge Pedestal Width of H-mode Plasmas in JT-60U", in JAERI-Research 97-047 (1997).

[2.3-6] Takizuka T. and ITER Confinement Database and Modelling Expert Group, 16th IAEA Fusion Energy Conference, Montreal, (1996) IAEA-CN-64/F-5.

2.4 Current Drive Experiments

2.4.1 Neutral beam current drive (NBCD) [2.4-1]

Non-inductive current drive by the newly installed negative-ion-based neutral beam injector (N-NBI) has been demonstrated at beam energy of 350 keV. Up to 0.28 MA of plasma current was driven by N-NBI. The current drive efficiency of N-NBI defined by $\eta_{CD} = n_e I_{CD} R_p / P_{CD}$, where n_e, I_{CD}, R_p and P_{CD} being respectively average electron density, non-inductively driven current, plasma major radius, and power of the current driver, reached 0.8×10^{19} $m^{-2}A/W$. This value is 1.6 times higher than that of conventional positive-ion-based NBI (P-NBI) at 80 keV and consistent with the theoretical prediction.

The JT-60U's N-NBI was designed to deliver 10 MW of beam power at 500 keV for 10 s. Up to now 2.5 MW of N-NB power has been injected into plasmas at beam energy of 350 keV.

Non-inductive driven current and current drive efficiency of N-NBI were evaluated by injecting N-NB into P-NBI heated plasmas (with 4 MW of tangential and 4 MW of perpendicular beams). An example of such discharge is shown in Fig. 2.4.1-1. Before the N-NB pulse, 70% of plasma current was driven by P-NB and the bootstrap current. During 2 MW of N-NB pulse, the neutron emission rate S_n increased by a factor of 2 and the loop voltage V_l became slightly negative indicating that the plasma current was driven fully non-inductively. With the aid of a 1.5-dimensional time-dependent tokamak transport analysis code TOPICS and a current drive code ACCOME, the bootstrap, P-NB, and N-NB driven currents were estimated to be 0.27, 0.46, and 0.28 MA, respectively.

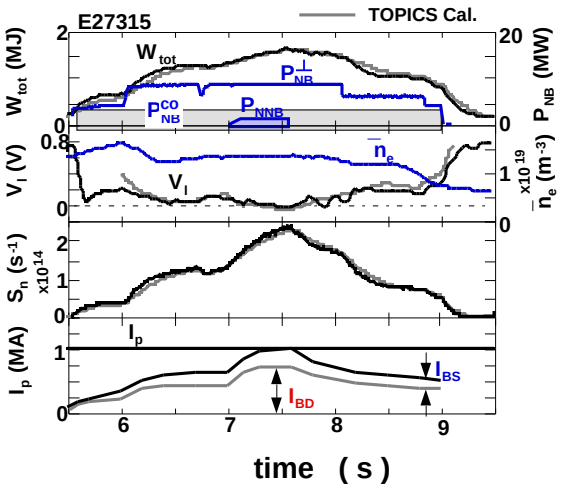

Fig. I.2.4-1 Time evolution of full non-inductive discharge by P-NB and N-NB. Total stored energy W_{tot}, NB power P_{NB}, loop voltage V_l, average density n_e, neutron emission rate S_n, plasma current I_D are shown.

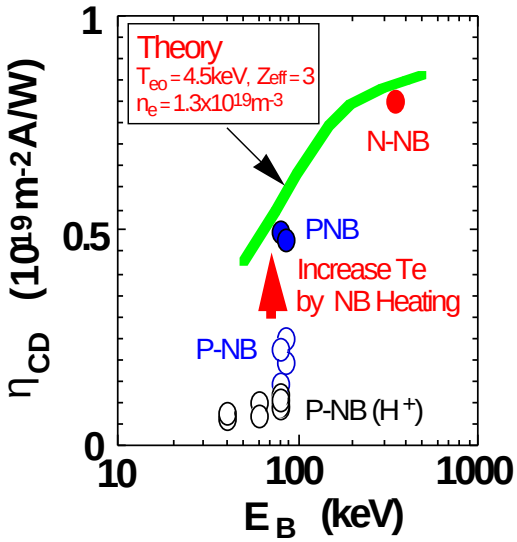

Fig. I.2.4-2 Current drive efficiency η_{CD} of NBCD as a function of beam energy E_B.

Figure 2.4.1-2 shows the current drive efficiency η_{CD} as a function of injected beam energy *EB*. Clearly, N-NB has efficiency higher than that of P-NB. The curve shows η_{CD} calculated

by ACCOME code with central electron temperature T_{e0} = 4.5 keV, effective ionic charge Z_{eff} = 3, and n_e = 1.3×10^{19} m–3. The experimentally obtained data are in reasonable agreement with theoretical prediction.

2.4.2 Lower hybrid current drive (LHCD) [2.4-2.2.4-3]

Current profile control by lower hybrid wave (LHW) was applied to the reversed shear plasmas. It has been demonstrated that the reversed shear configuration, otherwise relaxes to a monotonic shear profile, can be maintained by LHCD. It has also been shown that strong reversed shear with large area of shear reversal can be formed by LHW alone. The attainable normalized beta of such discharge is comparable to that obtained by current ramp-up method, and strong gradient is found in the electron temperature profile suggesting the improvement in confinement.

References

[2.4-1] Ushigusa K. and the JT-60 Team, to appear in Proc. 16th IAEA Fusion Energy Conf., Montréal, 1996, F1-CN-64/O1-3.

[2.4-2] Ide S., Naito O., Fujita T., *et. al.*, to appear in Proc. 16th IAEA Fusion Energy Conf., Montréal, 1996, IAEA-CN-64/E-3.

[2.4-3] Ide S., Fujita T., Naito O., *et. al.*, Plasma Phys. Controlled Fusion, **38**, 1645 (1996).

2.5 Radiative Divertor and SOL

2.5.1 Radiative divertor formation in the reversed shear plasma [2.5-1, 2]

The reversed shear plasma with an Internal Transport Barrier (ITB) has a potential to satisfy the target plasma conditions for a fusion reactor design. The radiative divertor formation with the improved energy confinement in the core plasma is a crucial requirement, and it was demonstrated for the first time in the reversed shear plasma. Full detached divertor condition was obtained for the reversed shear plasma (I_p = 1.2 MA, B_t = 3 T, P_{NBI} = 10-15 MW) with the ITB using a combination of neon and deuterium/hydrogen gas puffing. Total radiation loss power was increased up to 80% of the net input power for the central n_e = 4x10^{19} m^{-3}. The improved energy confinement within the ITB was maintained during the divertor MARFE for 3 sec. The results were the first demonstration of the compatibility of the radiative divertor with the ITB formation in the core plasma. The ITB was terminated by a beta-collapse during NB heating for the case of the deuterium (including neon impurity) plasma, while it was maintained for the case of the hydrogen plasma. An optimization of the gas puff sequence and the feedback control of the input power are required for the steady-state operation of the improved confinement plasma. During the sustainment phase of the ITB, the location of the minimum-q and the ITB shifted to the plasma center with the time constant of the current diffusion. The sustainment of the current profile is another important problem for realizing the steady-state operation.

2.5.2 Energy and particle confinement in high density ELMy H-mode

High density operation of the ELMy H-mode plasma has been performed in 1994-1995. Degradation of energy and particle confinements under the high recycling condition was investigated for high power neutral beam injection of 18-19 MW [2.5-3]; plasma parameters were fixed at I_p = 1-1.2 MA, B_t = 2-2.1 T, q_{95} = 3.3-3.5. The global energy confinement time τ_E and the H-factor H (compared with the ITER-89P scaling law for the L-mode) were reduced with increasing the plasma density n_e, which was caused by the decrease in the stored energy of fast ions due to a reduction in T_e. Here the thermal plasma energy was constant even for the increase in n_e. Global particle confinement time τ_p^G was evaluated using a neutral transport code for the divertor/SOL region, and it was found that τ_p^G greatly decreased from 0.13 to 0.08 s with increasing n_e due to an increase in the neutral particle influx from the divertor. Thus τ_p^G/τ_E decreased from 1.0 to 0.8 with increasing n_e for the ELMy H-mode plasma. This τ_p^G/τ_E is larger than that for the ELM-free H-mode plasma by a factor of 2-4, which is more favorable for achieving a cold and dense divertor plasma.

The increase in the neutral particle density inside the separatrix, n_0, was evaluated under the high density divertor condition. The n_0 near the X-point increased up to ~2×10^{16} m^{-3}, and it was by a factor of 10 larger than that at the midplane due to i) the short distance between the X-point and the divertor target plate and ii) the open divertor configuration. The transport of the neutral particles was calculated for the new (W-shaped) divertor configuration [2.5-4], which predicted that the inclined divertor plates and a dome in the private region can condense neutral particles in the divertor region. The effective formation of a dense and cold divertor plasma and the reduction of the neutral particles back-flow to the main plasma were also predicted, which will be investigated with their effects on the main plasma performance from 1997.

2.5.3 High density SOL plasma

Radial profiles of electron density at the midplane $n_{e,mid}$, temperature $T_{e,mid}$, and ion temperature $T_{i,mid}$ in the scrape-off layer (SOL) were investigated under radiative and detached divertor conditions in L-mode discharges (P_{NBI} = 4 MW) [2.5-5]. $T_{e,mid}$, and $n_{e,mid}$ profiles were measured with a fast reciprocating Langmuir probe. $T_{i,mid}$ profile at the edge was measured with charge exchange recombination spectroscopy system. The ratio of $T_{i,mid}/T_{e,mid}$ was found to be about 3 over a wide range of the plasma density, and the ion pressure was dominant. It was expected that $T_{i,mid}$ is higher than $T_{e,mid}$ due to the low parallel thermal conductivity of ion. The measured value of $T_{i,mid}/T_{e,mid}$ ~3 was consistent with the SOL/divertor two-point model.

Two (i.e. first and second) SOL regions with different characteristic lengths were measured both in the $n_{e,mid}$ and $T_{e,mid}$ profiles. The first SOL extended up to 10-15 mm outside the separatrix, where the parallel conduction is dominated. The profile had a small e-folding length. Effect of the connection length (safety factor) on the decay lengths of $n_{e,mid}$ and $T_{e,mid}$ (λ_{ne} and

λ_{Te}) was investigated. A regression analysis suggested that large dependence on the safety factor such as $\lambda_{ne} \sim q^{\alpha} T^{\beta}$, where $\alpha = 0.85$ and $\beta = 0.23$. λ_{Te} was larger by a factor of 1.5-2 than λ_{ne}, and λ_{Ti} was larger by a factor of 2.5-3 than λ_{Te} at the first SOL.

At the occurrence of the X-point MARFE, $T_{e,mid}$ at the separatrix was observed at 40-45 eV. During the X-point MARFE, λ_{Te}, λ_{ne} and λ_{Ti} increased substantially with a reduction in $T_{e,mid}$ and $n_{e,mid}$ at the plasma edge and in the first SOL. This is caused by the penetration of the intense radiation region into the main plasma near the X-point.

Parallel current $J_{//}$ flowing between the two strike points through the SOL was measured with the divertor Langmuir probes [2.5-6]. Location of the maximum $J_{//}$ corresponded to that of the peak of the ion flux Γ_{ion}. During the partial detachment of the divertor plasma, the locations of the peak $J_{//}$ and Γ_{ion} shifted from the separatrix to the outer magnetic flux surface. At the same time, the direction of $J_{//}$ was reversed due to the reversal of the in-out asymmetry in T_e profile. Thus not only Γ_{ion} but also $J_{//}$ changes the flowing root at the upstream during the divertor detachment.

References

[2.5-1] Itami K., Hosogane N., Asakura N. at al., Phys. Rev. Lett. 78, 1267 (1997).

[2.5-2] Itami K., Hosogane N., Asakura N. at al., to be published in Proc. 16th Int. Conf. on Plasma Physics and Controlled Nuclear Fusion Research, Montreal Canada, 1996, IAEA-CN-64/A-4-2.

[2.5-3] Asakura N., Koide Y., Shimizu K. et al., to be published in Plasma Phys. Control. Fusion, 1997.

[2.5-4] Hosogane N., Sakurai S., Shimizu K. et al., to be published in Proc. 16th Int. Conf. on Plasma Physics and Controlled Nuclear Fusion Research, Montreal Canada, 1996 IAEA-CN-64/GP-11.

[2.5-5] Asakura N., Koide Y., Itami K. et al., J. Nucl. Matter. 241-243, 559 (1997).

[2.5-6] Kumagai A., Asakura N., Itami K. et al., to be published in Plasma Phys. Control. Fusion, 1997.

2.6 Particle Confinement and Impurity Behavior

2.6.1 Particle confinement [2.6-1]

The density in the main plasma is maintained by not only the particle source in the main plasma but also the edge density. In order to understand the effects of the particle source distribution and the edge density on the global particle confinement, the local particle transport has been analyzed for L-mode plasmas. In this analysis, the densities maintained by the NBI source (n^{NB}) and wall-recycling source (n^{R}) and the base density (n^{Base}) were separated. Here, "base density" indicates the density that is not related with the particle source in the main plasma. The confinement times of the particles fueled by NBI (τ_p^{NB}) and that of the wall-recycling particles (τ_p^{R}) were estimated.

From the analysis in the steady state phase and the perturbed phase, the particle diffusion coefficient was estimated to be 1.0 m^2/s at the plasma edge and 0.1 m^2/s at the plasma center, and a large inward pinch velocity of 20 m/s was also obtained at the plasma edge. Using these estimated transport coefficients n^{NB}, n^{R}, and n^{Base} were separated. It was found that the base density is larger

than the other densities in all the plasma region and dominant at the edge region. The contributions of n^R, n^{NB} and n^{Base} to the total particle number were estimated to be 0.18, 0.22 and 0.6, respectively. τ_p^{NB} and τ_p^R were estimated to be 0.35 s and 0.14 s, respectively, and the ratio of τ_p^{NB} to τ_p^R was estimated to be 2.5. It was also found that τ_p^{NB} was not so large compared with τ_p^R although the penetration for the NBI source was about 10 times deeper than that for the wall recycling source. The high edge density and the large inward pinch gave the small τ_p^{NB} / τ_p^R.

Previously, τ_p^{NB} and τ_p^R had been estimated to be 0.9 s and 0.3 s from the analysis of the global particle balance, in which the base density had not been taken into account. The ratio of τ_p^{NB} to τ_p^R estimated from the global analysis was in agreement with the results obtained from the local analysis. However, τ_p^{NB} and τ_p^R estimated from the local analysis were smaller by 60% than those estimated from the global analysis. These results indicated the particle confinement can not be estimated from the particle number and the particle source in the main plasma. The base density should be considered for the investigation of the particle balance.

2.6.2 Active Control of Helium Ash Exhaust and Transport Characteristics[2.6-2]

In-out asymmetry of He flux in the divertor during the ELMy H-mode has been studied by scanning neutral beam power (PNB) and plasma current (Ip). The dependence of He exhaust on the ion grad-B drift direction, the plasma current and the toroidal magnetic field (BT) was investigated for the ELMy H-mode and L-mode. The He flux on the outer target was larger than that on the inner target in the cases of Ip = 1.0 MA, BT = 2.5 T, PNB = 18 MW. On the other hand, the He flux on the inner target was larger than that on the outer target in the case of Ip = 1.7 MA, BT = 3.5 T, PNB = 18 MW. The in-out asymmetry with the enhanced outboard He flux was remarkable for the ELMy H-mode with higher NB power heating and lower Ip. The in-out asymmetry of the He flux did not depend on the ion grad-B drift direction. However, the in-out asymmetry of the D flux could be reversed by the change of the ion grad-B drift direction (reversed BT and Ip). The asymmetry seemed to be determined by βp (including edge parameters: ne, Te, Ti et al.). It did not explicitly depend on NB power and Ip. This result suggested that the selective exhaust, for example He ash removal from the outboard divertor and fueled particle removal from the inboard divertor, may be possible.

Helium transport characteristics in reversed shear plasmas has been studied using a He beam (central fueling) and a short pulse He gas puff (edge fueling). In the reversed shear mode, the confinement is remarkably enhanced inside the internal transport barrier (ITB), which is formed near the position of minimum q. ne(r), Te(r) and Ti(r) profiles have large gradients at the ITB. The He particle confinement in the ITB was improved with the energy improvement. The He transport was found to be characterized by a large inward velocity near the ITB. However, the profile of He concentration (the ratio of the He density to the electron density) in reversed shear plasmas was almost flat because the electron density profile was similar to the He density profile.

The transport in the reversed shear mode is clearly different from that in the ELMy H-mode and L-mode. However, He particles inside the ITB was expelled when a partial collapse occurred as observed for ELMs. It suggested that Helium can be removed from reversed shear plasmas by frequent partial collapses.

2.6.3 Behavior of Neutral Deuterium and Helium Atoms in the Divertor Region [2.6-3, 4]

Understanding of behavior of neutral deuterium and helium atoms in divertor regions is necessary to control fueling and pumping in fusion plasmas. In the divertor region, the Doppler broadening of Dα and He I (667.8 nm) lines has been observed and analyzed to study the recycling and emission processes of neutral deuterium and helium atoms.

The Dα line profile was observed with wavelength resolution of 0.011 nm; this wavelength resolution corresponds to the temperature of deuterium atoms of 0.09 eV. The profile was simulated with a two-dimensional neutral particle transport code (DEGAS) using the electron temperature and density measured by Langmuir probes at the divertor tiles. The measured Dα line profile was well reproduced by this simulation, which showed that it is necessary to consider the emission from deuterium atoms excited at dissociation of deuterium molecules and ions. It was found that the reflection model using reflection coefficients overestimated the reflection of deuterium atoms at the surface of the divertor tiles by a factor of 2 - 3.

The profile of He I line was observed with wavelength resolution of 0.014 nm; this wavelength resolution corresponds to the temperature of helium atoms of 0.29 eV. In low-density divertor plasmas, the width of the observed He I line was close to the wavelength resolution, which suggested that the helium atoms are dominantly desorbed with the energy of the surface temperature of the divertor tiles. As the electron density of divertor plasmas increased and the electron temperature of them decreased, the line width increased. The temperature corresponding to the width of He I line was 1.7 eV for partially detached plasmas. Since it is expected that the helium atoms with such high energy significantly affect helium contamination of the main plasma and the pumping efficiency of He ash, it is important to understand the production mechanism of atoms with the high energy. It was shown that the heating of the helium atoms by the elastic collision with deuterium ions can qualitatively explain the mechanism.

References

[2.6-1] H. Takenaga, K. Nagashima, N. Asakura et al., "Effects of Source Distribution and Edge Density on Particle Confinement in JT-60U", to be published in Nucl. Fusion (1997).

[2.6-2] A. Sakasai, H. Kubo, K. Shimizu, et al., "Active Control of Helium Ash Exhaust and Transport Characteristics in JT-60U", Proc. of the 16th Int. Conf. on Plasma Phys. Control. Nucl. Fusion Res., Montreal, O2-6, AP-2-1 (R), (1996).

[2.6-3] H. Takenaga, H. Kubo, T. Sugie, et al., "Neutral deuterium and helium behavior in JT-60U divertor plasmas", Proc. 1996 Int. Conf. on Plasma Physics, Nagoya, **1** 642 (1997).

[2.6-4] H. Kubo, H. Takenaga, T. Sugie et al., "Behavior of Neutral Deuterium and Helium Atoms in the Divertor Region of JT-60U", Proc. 24th EPS Conf. on Controlled Fusion and Plasma Physics, Berchitesgaden, (1997).

2.7 Fast Ion Study in ICRF Heating

In JT-60U, second harmonic ICRF minority heating of deuterium plasma in negative shear discharges was found to efficiently heat bulk plasmas inside the transport barrier. The plasma stored energy, the electron and ion temperatures in the plasma core remarkably increased after the onset of the ICRF injection and reached 5 MJ, ~7 keV and ~12 keV, respectively.[2.7-1] However, in reversed magnetic shear plasma, fast ion confinement is anticipated to be deteriorated because of weak poloidal magnetic field in the core. The JT-60U experiment indicated that confinement of energetic ions in reversed magnetic shear was inferior to that in the normal shear with positive magnetic shear. The experimental triton burnup ratio in the reversed shear was a half or a third of the expected, while that in the normal shear almost agreed with the calculation. The results indicate that a significant fraction of energetic tritons escaped from the plasma in the reversed shear, raising a concern on serious losses with MeV class ions in reversed shear operations of steady state tokamak reactors. Stochastic and collisional ripple losses are a probable explanation for the significant triton losses. [2.7-2] Toroidicity-induced Alfvén eigen (TAE) modes excited by ICRH were studied in a low-q plasma. Low shear TAE modes and bi-directional TAE modes were observed for the first time. In the low-q discharge similar to ITER configuration it is found that the location of TAE modes shifted from the outside to the inside of the q=1 surface following the expansion of the q=1 surface caused by current diffusion into core region accompanying decrease of li. The higher order TAE modes inside q=1 surface (tornado modes) are much more harmful for energetic ion confinement than the TAE modes outside q=1 surface.[2.7-3] The TAE mode, the ellipticity induced Alfvén mode (EAE) with mode number m and m+2 and the noncircular induced Alfvén eigen mode (NAE) were observed for the first time by means of Mirnov coil in the NBI and ICRF heated plasma of JT-60U [2.7-4].

Diagnostics of the highly energetic α-particles created by the D-T fusion reactions are necessary in a fusion reactor tokamak. Ion Cyclotron Emission (ICE) is one of the simplest and most promising diagnostics. It consists in measuring the radiation emitted by the ions rotating around the magnetic field lines at the first harmonics of cyclotron frequency (f ~ 10-200 MHz). The radiation detected is principally due to the fast ions, even if they are in a very small minority in comparison with the thermal ions. In an NBI-heated plasma, the perpendicular electric field spectra are consisted of narrow, regularly spaced peaks. Their frequencies correspond to the cyclotron harmonics of the main ion species taken at the plasma outer edge. In high βp discharges we detect emission peaks corresponding to the first three cyclotron harmonics of fusion tritons at the plasma center (R ~3.1-3.2 m) in a tokamak for the first time. The measurement of ICE during ICRF heating shows the redistribution of the emission peaks due to parametric instabilities. We observe good correlations between ICE at fixed frequencies and ELMs. We also observe oscillations in ICE due to the expulsion of fast ions from the plasma center during fishbone-type instabilities. We do not observe any evidence of correlation with TAE modes.[2.7-5]

References

[2.7-1] H. Kimura et al., Proceedings of the 16th IAEA Fusion Energy Conference, Montreal, 1997, paper F1-CN-

64/E-6 (IAEA, Vienna, to be published).
[2.7-2] K. Tobita, T. Nishitani, H. Harano, K. Tani, M. Isobe, et al., in Plasma Physics and Controlled Nuclear Fusion Research 1996 (Proc. 16th Int. Conf. Montreal, Canada 1994), IAEA, paper IAEA-CN-64/A5-6.
[2.7-3] M. Saigusa et al., Plasma Phys. Control. Fusion Res., 37, 295 (1995).
[2.7-4] G.J.Kramer et al., submitted to Phys. Rev. Lett.
[2.7-5] O. Da Costa et al, International Conference on Plasma Physics, Nagoya, 1996.

2.8. Plasma Control and Disruption

The fast current shut down scenario using the killer-pellet injection (KPI) has been demonstrated without the generating harmful runaway electrons (REs) in JT-60U. The "burst" like magnetic-fluctuations are enhanced by external helical magnetic-fields. The enhanced magnetic fluctuations can eliminate the relatively low-energy super-thermal (slideaway) electrons created just after the KPI, consequently the quick generation of REs which cause current tail is suppressed. [2.8-1]

In the experimental condition of NB power 32 MW, Ip=2.2 MA and Bt=4.1 T, in JT-60U, during ELMy H-mode phase, some of giant ELMs cause a plasma displacement, which mainly moves in the vertical direction over a maximum distance of ~ 4.7 cm. A large vertical displacement (VD) of ZJ occurs at giant ELMs. This phenomenon can be divided into two phases based on plasma movement. In phase I, a small βp-drop and a small RJ-shift are observed while in phase II, a l_i-drop of by ~ 0.25 and a large ZJ-drop of by ~ 4.7 cm occur. And this large VD in phase II has been confirmed by the soft X-ray emission. The large VD is always observed with a large decrease in l_i. Intense n = 1 ~ 3 modes are always observed at the giant ELMs accompanied by the large VD, which would explain the sudden l_i-drop. It is necessary to clarify the mechanism of VD at giant ELMs and work out effective measures to cope with giant ELMs when they occur. Here, the vertical position of the Ip-center (ZJ) is measured from the mid plane of the vacuum vessel, and the horizontal position of that (RJ) is the plasma major radius. [2.8-2]

Extremely fast vertical displacement events (VDE's) induced by a strong β_p collapse were found in a vertically elongated (κ ~ 1.5), high β_p (β_p ~ 1.7) tokamak with a resistive shell through computer simulations using the Tokamak Simulation Code. Although the plasma current quench, which had been shown to be the prime cause of VDE's in a relatively low β_p tokamak (β_p ~ 0.2), was not observed during the VDE evolution, the observed growth rate of VDE's was almost five times (γ ~ 655 sec^{-1}) faster than the growth rate of the usual positional instability (γ ~ 149 sec^{-1}). The essential mechanism of the β_p collapse-induced VDE was clarified to be the intense enhancement of positional instability due to a large and sudden degradation of the magnetic field decay n-index in addition to the significant destabilization due to a reduction of the stability index ns. The radial shift of the magnetic axis caused by the β_p collapse induces eddy currents on the resistive shell, and these eddy currents produce a large degradation of the n-index.[2.8-3]

References

[2.8-1] Y. Kawano, et. al., paper IAEA-CN-64/A3-4 in 16th Fusion Energy Conference, Montreal (1996).
[2.8-2] OHSAWA M., et al., ICPP96,12E04
[2.8-3] NAKAMURA K., Plasma Phys. Control Fusion 38 1791 (1996)

3. Design Progress of the JT-60SU

To realize the steady-state tokamak reactor such as SSTR, simultaneous achievement is required at high q (5-6) and high β_p (2-2.5), in addition to the alpha burning, of (1) high energy confinement (H-factor>2) under good particle controllability, (2) stable high normalized beta (β_N~3.5), (3) high bootstrap current fraction and high efficiency non-inductive current drive, and (4) heat load reduction and He ash exhaust with divertor. The JT-60SU machine has been studied to establish such a reactor relevant operation mode using deuterium as well as to contribute to the advanced steady-state ITER scenario [3-1].

3.1 Key Design Features

Major parameters of the recent JT-60SU design are shown in Table I.3-1. Firstly, a low unit weight w =(weight/magnetic energy) of 125ton/GJ is realized for the TF SC (super-conducting) magnets as compared with w = 1000ton/GJ of JT-60U Cu magnets. Primary candidate for TF SC cable is Nb_3Al with its good mechanical property. Ten units of the PF coils, 6 EF coils and 4 CS coils, can produce a wide variety of plasma shaping of elongation κ_x up to 2.0 and triangularity δ_x up to 0.8 for DN divertor. The total magnet weight is ~4000ton and is cooled down to liquid He temperature (4.2 ^oK) with a 40kW cryogenic system. To allow a wide variety of current profile control, both NBI (750keV) and ECW (220GHz) are considered as heating and current driver because of their remote coupling capability to the plasmas. The total heating power is 60MW and is larger than the H-mode power threshold of ~40MW. Demonstration of 5MA full current drive is planned for 1000s-1Hr at $<n_e>$~$8.8\times10^{19}m^{-3}$ which is around the Greenwald density limit [3-2]. Full current drive of 6MA at β_N=3 could be tested if the D-T operation is allowed. A plasma current of 10MA can be driven inductively for 200 s. The power supply (P/S) for the SC PF coils utilizes the present JT-60 P/S and two motor generators. New water-cooled 280MW thyristor P/S is enough for a long pulse operation. The vacuum vessel is designed to have one-turn resistance of 25μΩ. The growth rate of the vertical instability γ and stability margin $m_s=(n_s(\infty)+n)/|n|$ are $\gamma \leq 30/s$ and $m_s \geq 0.5$, respectively, with toroidally continuous divertor baffle plate. Active control coils are located between TF coils and the vacuum vessel.

3.2 Safety Issues

Material selection of the vacuum vessel is one of key issues to improve safety and to reduce the exposure dose. Feasibility of SUS316 with low cobalt concentration (0.05%) is studied. Inner wall is covered with 3cm W shield in order to allow human access inside the vessel, even after 1 year cooling down followed 10 years of high power deuterium experiments (with DD neutron production of 4×10^{22}/year). Total weight of the vacuum vessel is ~1600ton. In case of possible future DT operation, an additional-shield of ~2400ton (reduced activation ferritic steel F82H) is required. Radiation shield against DD neutrons and induced γ-rays consists of vacuum vessel

(40cm thick) and cryostat (50cm thick) to reduce the radiation dose rate at the site boundary. Additional shield inside the vacuum vessel and TF magnet with polyethylene blocks filled inside the TF shear-panel are enough to keep the radiation dose of the DT option to that for DD experiments. Tritium production from intense auxiliary heating of deuterium plasma is estimated to be 2000Ci/year. The fuel treatment and tritium removal systems are planned to have multiple confinement barriers and defense-in-depth philosophy, similar to the tritium process laboratory (TPL) at JAERI.

References

[3-1] M. Kikuchi et al., IAEA-CN-64/G-2-3(1996).

[3-2] K. Nagashima et al., to be published in Fusion Engineering and Design.

Table I.3-1 Major parameters of JT-60SU

Plasma current	10	MA	Flux swing	170V s	
Toroidal field at 4.8m	6.25	T	Divertor pumping	$20Pam^3/s$	
Plasma major radius	4.8	m	DD neutron rate	$1x10^{18}/s$	
Plasma minor radius	1.4	m	Elongation (κ_{95})	1.8	
Triangularity (δ_{95})	0.4		Inductive flat top	200s	
Heating power(NBI & ECH)	60	MW	Non-inductive pulse	1-1000hr	
TF magnet energy	24	GJ			

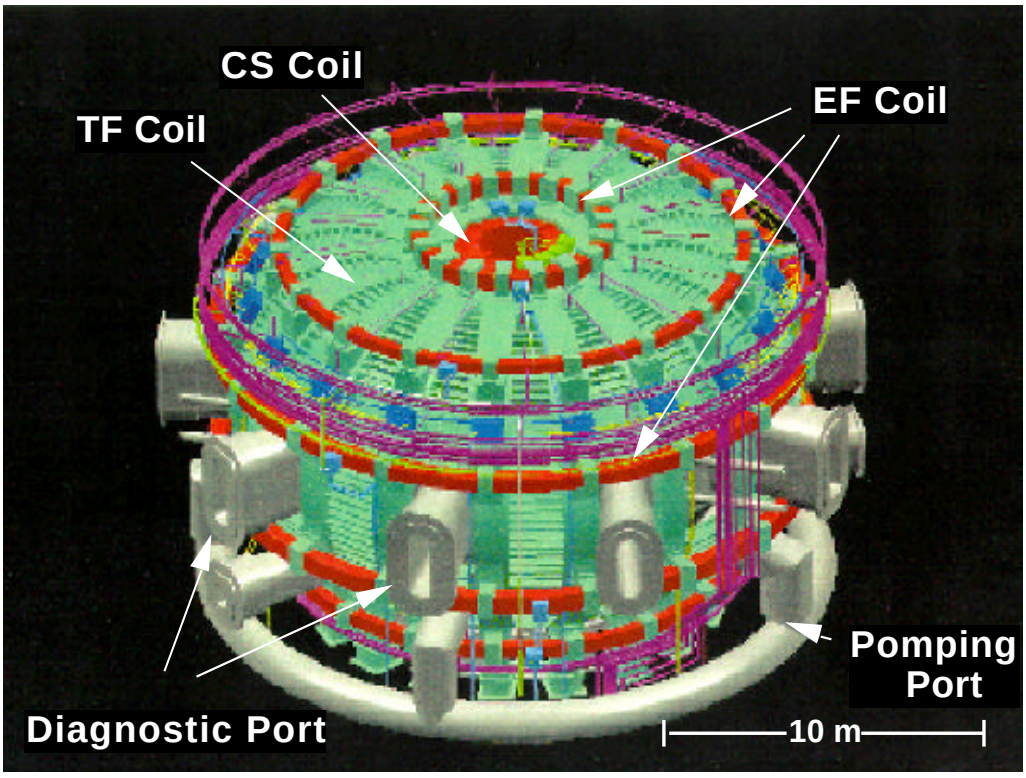

Fig.I.3-1 Birds' eye view of the JT-60SU

II. JFT-2M PROGRAM

Objectives of the JFT-2M program are (1) advanced and basic researches for the development of high-performance plasmas for nuclear fusion and (2) contribution to the physics R&D for ITER, with a merit of flexibility of a medium-size device (R=1.3 m, a=0.35 m, B_T=2.2 T and I_p=0.5 MA). Both international and domestic collaborations have been vigorously utilized to strengthen activities of JFT-2M. In the last fiscal year, the baffle structure for the closed divertor had been modified to have more closed geometry. In this fiscal year, the modified closed divertor was found to be more effective for compatibility of the H-mode and the dense and cold divertor plasma. Physics studies on H-mode also made progress, such that a region of suppression of the density fluctuation was found to coincide with that of a high shear region of the radial electric field. It was demonstrated that the m=2 tearing mode was suppressed by the O-mode ECH for the first time in an elongated plasma. Plasma coupling experiment of the combline antenna for FWCD was carried out in collaboration with General Atomics, demonstrating merit of load insensitivity of the antenna. Planning of the Advanced Material-Tokamak Experiments (AMTEX) was initiated, which will provide database on effects of ferritic material on tokamak plasma, including toroidal field (TF) ripple reduction. In this fiscal year, water leakage occurred at the inlet of cooling water to one of the TF coils. Replacement of all the inlet and outlet connectors to the TF coils with new-type ones has been completed within this fiscal year.

1. Experimental Results and Analyses

1.1 Closed Divertor

Handling of the heat load onto a plasma facing component, e.g. divertor plate, for a fusion reactor keeping the plasma in high confinement state is still an open question. One of the promising examples to solve this question is the dense & cold divertor which we found in D-III open divertor. But it was in L-mode due to high recycling and restricted in high density regime [1.1-1].

Our target had been to realize dense & cold divertor plasma and H-mode simultaneously, employing a closed divertor. It is expected that the closed divertor reduces recycling at the main plasma edge, keeping high recycling in the divertor region. The effect of baffle plate opening on neutral gas back flow from the divertor chamber had been examined. The shape of the baffle plates had changed from less closed configuration (CD1) to more closed configuration (CD2) in March, 1996. The edge of the outer baffle plate is located near the X-point at the position about 1.4 λ_Γ and 0.8-0.9 λ_Γ from the peak position of the particle flux profile near the divertor throat for CD1 and CD2, respectively, where λ_Γ is an e-folding length of the particle flux profile. In addition, the gap between inside hit point and the baffle plate for the private region was reduced from about 5cm to 2cm. In order to compare the baffle effect on the simultaneous realization of

a dense & cold divertor plasma and an H-mode, we tried to increase a gas feed rate, Q_H, shot-by-shot into the divertor chamber. Note that the gas was introduced after the H-mode transition for the low target density case where the spontaneous dense & cold state disappears. In CD1, the H-mode was compatible with a dense & cold divertor to some extent, but was degraded and then terminated when Q_H exceeds 2.8 Pam^3/s [1.3-2]. The divertor plasma was not enough cold (~15eV). With the reduced baffle opening in CD2, buildup of gas was established only in the divertor chamber to the extent of Q_H = 4.0 Pam^3/s without degrading H-mode [1.3-3]. Principal parameters at 100 ms after the beam initiation are shown in Fig. II.1.3-1. The divertor plasma is becoming much denser and colder (Fig. II.1.3-1(a)) compared to those of CD1 in accordance with sole buildup of neutral gas pressure in the divertor chamber while the main chamber pressure kept low by increasing of Q_H (Fig. II.1.3-1(d)). Neutral compression ratio (divertor pressure/main pressure: an index of baffling performance) exceeds 35. This ratio is doubled by applying divertor biasing.

Since the strong Q_H gives less affection on the main plasma parameters, i.e. electron density, plasma stored energy, radiation/charge-exchange loss power and neutral gas pressure as shown in Figs. II.1.3-1(b)~(d), we would say that the gas puffing from the closed divertor chamber has a capability of controlling dense & cold states independently of the main plasma even in H-mode. The suppression of the gas buildup of main chamber by a divertor shape optimization, which we have firstly shown experimentally, is the necessary condition of the divertor design for ITER.

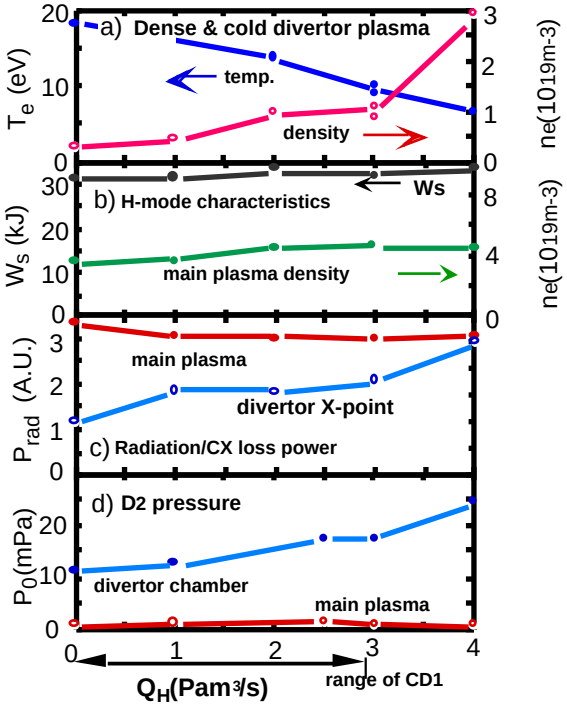

Fig. II.1.1-1 Main parameters during H-mode against gas feed rate, Q_H, a) electron temperature and density at the divertor plate, b) line averaged electron density and stored energy, c) radiation/CX loss power in the main plasma and the divertor X-point region, d) deuterium neutral pressure in divertor and main plasma periphery. P_{NBI} ~ 0.7 MW, B_T = 1.3 T and I_p ~ 220 kA.

References

[1.3-1] S. Sengoku, M. Shimada, N. Miya et al., Nucl. Fusion, **24**, 415 (1984).
[1.3-2] S. Sengoku and the JFT-2M group, Bull. Amer. Phys. Soc., **40**, 1765 (1995).
[1.3-3] S. Sengoku and the JFT-2M group, Bull. Amer. Phys. Soc., **41**, 1486 (1996).

1.2 Confinement Studies

Understanding the relation between the transport and the micro turbulence is one of the most important topics in the fusion plasma research. In JFT-2M, the turbulence is measured by a

microwave reflectometer technique. The reflectometer installed on JFT-2M is a 2 channel heterodyne system. The frequency of the launching waves can be tuned from 28 to 50GHz. The polarization of the wave is O-mode, so that the corresponding cut-off density is from 0.97 to $3.1\times10^{19}m^{-3}$. This range of density lies in the region of $0.5<r/a<1$ in a typical L-mode and $0.9<r/a<1$ in a typical H-mode. In the analysis, we consider that the received wave has two component at least. One is the reflected wave coming from the geometrical optics and the other is the waves scattered by the density fluctuations. This consideration allows us to analyze the density fluctuation by taking a complex spectrum under the runaway phase phenomenon [1.2-1].

Figure II.1.2-1 shows a temporal evolution of power spectra of the complex amplitude at an L/H transition. The fluctuations coming from the cut-off layer of $1.83\times10^{19}m^{-3}$ (inner cut-off) and $0.97\times10^{19}m^{-3}$ (outer cut-off) are shown in Fig.II.1.2-1(b) and Fig.II.1.2-1(c), respectively. The L/H transition occurs at 731 ms (from the reduction of D_α intensity shown in Fig.II.1.2-1(a)). The density fluctuation with frequency lower than about 100 kHz at the outer cut-off layer was reduced at the time of the L to H transition, while the density fluctuation at the inner cut-off layer was reduced with the delay of about 20 ms after the L to H transition. Figure II.1.2-1(d) shows the movement of the inner and outer cut off layers that are obtained by using the numerical low pass filter. The delay time of reduction of the fluctuation at the inner cut-off layer from the L/H transition might be the time to reach its position to the high shear of the radial electric field region [1.2-2]. It may support the model of the turbulence stabilization by an E×B induced poloidal flow.

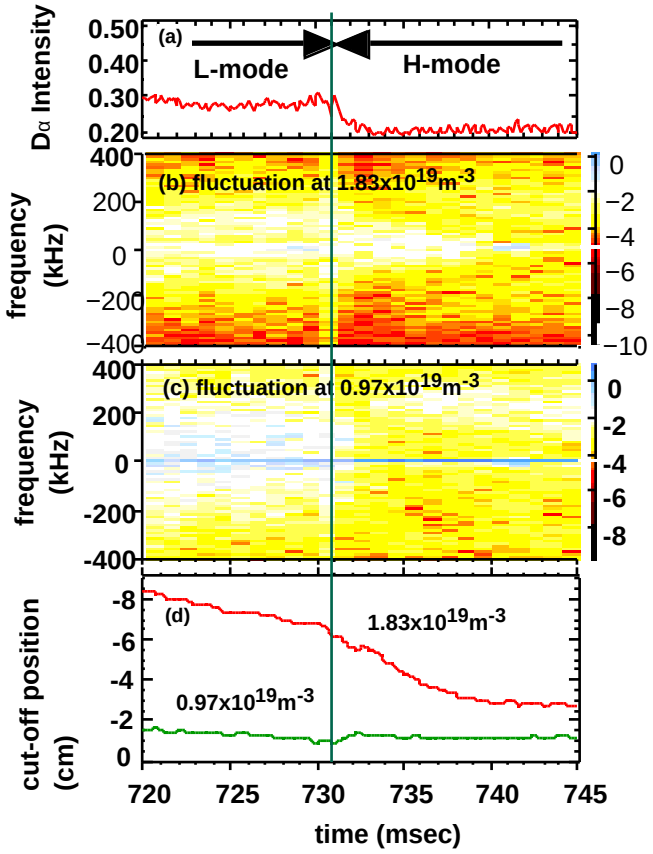

Fig.II.1.2-1 (a); D_α intensity. (b) and (c); Power spectra of the complex amplitude in logarithmic-scale (the more dark shows more week of the amplitude). (d); Movement of the inner and outer cut-off layer. The vertical axis shows the position of the cut-off layer from the separatrix. The sign of this axis is negative inside the separatrix.

References

[1.2-1] G.R.Hanson et al., Nucl. Fusion **32**, 1593 (1992).

[1.2-2] K.Ida et al., Phys. Fluids **4**, 2552 (1992).

1.3 Disruption Control by ECH

The power of the ECH system of the JFT-2M was increased up to 1MW in the last fiscal year in collaboration with the United States. The first ECH experiment after the power-up was carried out in this year. For the tokamak plasma of circular cross-section, we already found that avoidance of the disruption is possible by the local island heating of the tearing mode using the off-center heating by ECH [1.3-1,2]. We used the 2nd harmonic X-mode in those experiments.

In this year, we launched the fundamental O-mode into the elongated diverted plasma whose configuration may be realistic for a future thermonuclear fusion reactor. We found that the m=2 tearing mode which was observed in the single null divertor discharge (q_{95}=4.8, ellipticity=1.46, triangularity =0.42), was found to be suppressed by the off-central-heating (net power =0.2 MW), for the first time in such an elongated plasma [Fig. II.1.3-1]. The O-mode, whose single path absorption is less than the 2nd harmonic X-mode, was found to be effective for the suppression of the mode. We plan to continue the study with plasmas of larger plasma current and lower q value. Furthermore, we achieved the electron temperature of 2.5-3.0 keV, which is the highest value in JFT-2M, by the central heating (power=0.25 MW, line averaged density =1.1x$10^{19}$$m^{-3}$). Such a parameter region is the target for the current drive experiments with the 200 MHz fast wave. We will continue the conditioning to get the higher power and higher plasma temperature.

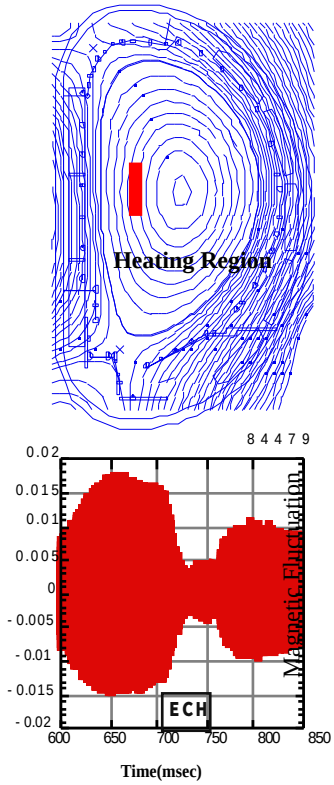

Fig. II.1.3-1 Suppression of the tearing mode by ECH in the diverted discharge with B_T= 1.87 T and I_p = 0.2 MA, Top: Magnetic surface at 0.725s, The heating position is 14 cm inside (plasma radius 27 cm). Bottom: Time evolution of the magnetic fluctuation (time derivative).

A localized current drive is possible by ECH. There is a possibility that we can avoid the tearing mode/disruption more effectively by the local current drive in the magnetic island of the tearing mode. It is expected that the current drive is dependent on the direction of the ray of the wave. In order to study the effect of the ray direction to the current drive, we designed a new launcher with mirrors, with which the ray direction can be changed. We did the engineering development in collaboration with the RF heating laboratory.

References

[1.3-1] K. Hoshino et al., Phys. Rev. Lett., **69**, 2208 (1992).

[1.3-2] K. Hoshino et al., in Radio Frequency Power in Plasmas, Boston 1993, AIP Conference Proceedings, **289**, 149 (1994).

1.4 Advanced Material - Tokamak Experiment (AMTEX) Program

Ferritic steel is one of the candidate materials for a DEMO fusion reactor, such as SSTR, because of its low activation under fast neutron irradiation. However, one concern is that their ferromagnetic properties would have harmful effects on plasma production, plasma control and confinement performance. In order to examine the effects, advanced material-tokamak experiments (AMTEX) are planned in JFT-2M. For AMTEX, the ferritic material F82H (8%Cr-2%W-0.2%V-0.04%Ta-Fe) [1.4-1] which has a low activation of 10^{-6} damping factor/century is considered. F82H begins to saturate at magnetic field strength (H)~ 0.2[MAT/m] and saturated magnetic flux density (B) is 2T with an external B of about 0.3T [1.4-2]. Although F82H is not saturated in low magnetic field discharge (for instance a Taylor discharge cleaning (B=0.07 T)), F82H is saturated in normal tokamak discharges (B≤ 2.2 T). The issues of AMTEX on JFT-2M are to clarify the effects of the ferritic steel on plasma production, plasma control and confinement property as well as plasma-wall interaction, and to obtain guidelines for the design of tokamaks with a small toroidal ripple. We have evaluated the error magnetic field from the ferritic steel by a computer simulation code. The magnetic field is calculated using a 3D static magnetic field analysis code ELF/MAGIC made by the ELF Corp.. The method is the same as that in the case of the SSTR [1.4-3]. If ferritic steel boards are located inside toroidal coils, they strengthen magnetic field between toroidal coils, while the toroidal magnetic field just inside the coils becomes weaker. Thereby, toroidal field ripple can be reduced. A ferritic board of 24 mm in thickness, 500 mm in height and 150 mm in width is assumed to be attached outside of vacuum vessel. The preliminary results in the case with and without ferritic steel board is shown in Fig.II.1.4-1. The ripple is significantly reduced in the plasma region in the case with ferritic steel boards.

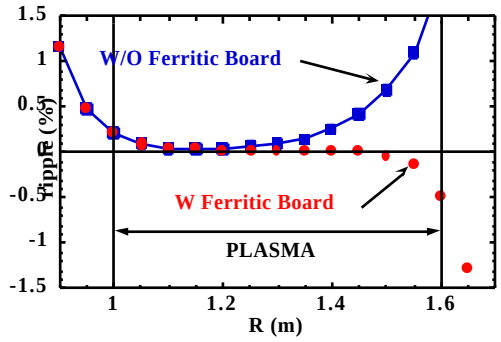

Fig.II.1.4-1 Ripple on the horizontal plane in the case with and without setting Ferritic board.

Reference

[1.4-1] M. Tamura *et. al.*, J. Nucl. Matter, **155**, 620 (1988).
[1.4-2] K. Siba and A Oyama, private communication
[1.4-3] S. Takeji *et. al.*, in Proc. of the 16th IEEE/NPSS SOFE, Illinois, **2**, 1214 (1995).

2. Operation and Maintenance

JFT-2M tokamak has been running for ITER physics R&D experiments. In this fiscal year, main apparatus (JFT-2M tokamak, heating apparatus and flywheel motor-generator for toroidal field coil) was smoothly operated from April to December according to the experimental plan. The total shots of 2249 were devoted to experiments on closed divertor, H-mode characteristics, electron cyclotron resonance heating and fast wave current drive. In the residual period, periodical

inspection and some repairing were carried out on each apparatus. Furthermore, a capacitor bank for the compact toroid injection was prepared, and technical problems to use ferritic steel on JFT-2M were discussed and basic design of plasma- materials test program has started.

2.1 Tokamak

Tokamak operation started in April after wall conditioning with baking and TDC. In May, small leak of cooling water from a joint to toroidal field coil was found, however, electrical insulation between coils and the earth was not degraded, so after temporary repairs tokamak operation was continued without 3 cooling channels. As main cause of water leak comes from superannuated seal material, regular examination and replacement of water joint for all toroidal coils were carried out in the periodical maintenance time. During closed divertor experiments, some troubles have occurred on electrical insulation of divertor plates by arcing, mineral-insulated cable disconnection by electro-magnetic force and current feed-through air leak by arcing, so preventive measures for each trouble have been taken in the maintenance time. In the vacuum system, old vacuum gages were replaced and a new He leak detector capable to distinguish He and D2 was installed. New experiments to inject a compact toroid into JFT-2M plasma has been planned and manufacture of the injector system has started in 2 year schedule by collaboration with Himeji Institute of Technology. Plasma-materials test program to support development of structure materials such as ferritic steel has started. Technical problems such as error field production, vacuum characteristics and electro-magnetic force were discussed and basic design of ferritic steel setup was decided.

2.2 Neutral Beam Injection System and Radio-Frequency System

Neutral beam injection system (NBI) has contributed to almost all experiments as a main heating apparatus. In order to reduce time needed for conditioning, a baking heater was newly installed on the manifold. Old vacuum pumps for NBI were replaced to new one. Electron cyclotron heating system(ECH) with maximum power of 1MW by 5 gyrotrons was adjusted to operate with long pulse by cooperating with GA technologies. These gyrotrons were applied to experiments on suppression of MHD fluctuation and current drive. Fast wave system with a comb-line antenna developed by GA technologies had been adjusted and experiments on coupling characteristics have been carried out before experiments on DIII-D.

2.3 Power Supply

DC generator with a flywheel which has capability of 51.3 MW through 4 seconds was operated smoothly and experiments on ECH have been carried out at 2.2 T. In the maintenance time, precise examination of main circuit switches were carried out to keep good conditions and a higher harmonics filter were added in the syristor circuit to reduce higher harmonics in the commercial line.

2. Operation and Maintenance

JFT-2M tokamak has been running for ITER physics R&D experiments. In this fiscal year, main apparatus (JFT-2M tokamak, heating apparatus and flywheel motor-generator for toroidal field coil) was smoothly operated from April to December according to the experimental plan. The total shots of 2249 were devoted to experiments on closed divertor, H-mode characteristics, electron cyclotron resonance heating and fast wave current drive. In the residual period, periodical inspection and some repairing were carried out on each apparatus. Furthermore, a capacitor bank for the compact toroid injection was prepared, and technical problems to use ferritic steel on JFT-2M were discussed and basic design of plasma- materials test program has started.

2.1 Tokamak

Tokamak operation started in April after wall conditioning with baking and TDC. In May, small leak of cooling water from a joint to toroidal field coil was found, however, electrical insulation between coils and the earth was not degraded, so after temporary repairs tokamak operation was continued without 3 cooling channels. As main cause of water leak comes from superannuated seal material, regular examination and replacement of water joint for all toroidal coils were carried out in the periodical maintenance time. During closed divertor experiments, some troubles have occurred on electrical insulation of divertor plates by arcing, mineral-insulated cable disconnection by electro-magnetic force and current feed-through air leak by arcing, so preventive measures for each trouble have been taken in the maintenance time. In the vacuum system, old vacuum gages were replaced and a new He leak detector capable to distinguish He and D2 was installed.

New experiments to inject a compact toroid into JFT-2M plasma has been planned and manufacture of the injector system has started in 2 year schedule by collaboration with Himeji Institute of Technology.

Plasma-materials test program to support development of structure materials such as ferritic steel has started. Technical problems such as error field production, vacuum characteristics and electro-magnetic force were discussed and basic design of ferritic steel setup was decided.

2.2 Neutral Beam Injection system and Radio-frequency System

Neutral beam injection system (NBI) has contributed to almost all experiments as a main heating apparatus. In order to reduce time needed for conditioning, a baking heater was newly installed on the manifold. Old vacuum pumps for NBI were replaced to new one. Electron cyclotron heating system(ECH) with maximum power of 1MW by 5 gyrotrons was adjusted to

operate with long pulse by cooperating with GA technologies. These gyrotrons were applied to experiments on suppression of MHD fluctuation and current drive. Fast wave system with a comb-line antenna developed by GA technologies had been adjusted and experiments on coupling characteristics have been carried out before experiments on DIII-D.

2.3 Power Supply

DC generator with a flywheel which has capability of 51.3 MW through 4 seconds was operated smoothly and experiments on ECH have been carried out at 2.2 T. In the maintenance time, precise examination of main circuit switches were carried out to keep good conditions and a higher harmonics filter were added in the syristor circuit to reduce higher harmonics in the commercial line.

III. THEORY AND ANALYSIS

The primary objective of theory and analysis is to improve the physical understanding of the magnetically confined tokamak plasma. Remarkable progress has been made on understanding of physics of the reverse shear plasma such as reduced transport near the pitch minimum location for "semi-global" toroidal turbulence, stability properties of ideal MHD, TAE and kinetic ballooning modes. Progresses are also made on understanding of VDE mechanism and nature of divertor asymmetry using 5 point divertor model. New Implicit Monte Carlo method is also developed for the analysis of impurity ionization and recombination. Selective He ash exhaust is also demonstrated using OFMC code simulation.

The main focus of the NEXT (Numerical Experiment of Tokamak) project is to simulate tokamak plasmas using particle and fluid models on the developing technology of massively parallel computers. For core plasmas, three models are being developed; a particle model, a fluid model, and a particle/fluid hybrid model. For the divertor, particle and fluid models are being developed. The NEXT project involves research in parallel computing technologies.

1. Confinement and Transport

It is understood that drift waves in a toroidal geometry behave quite differently from a slab geometry. In a toroidal geometry, excited eigen-modes are radially extended to a semi-global width given by $\Delta r \sim (\rho_i L)^{1/2}$ [1-1]. This originates from a toroidal geometrical effect which couples the small scale ion gyro radius ρ_i with a scale length L of the plasma equilibrium. This understanding leads to a strategy where improved modes can be achieved by suppressing such prominent structures. We have investigated the role of magnetic shear and plasma shear rotation on the improved modes using toroidal numerical simulation and theory [1-2]. We found that the weak and/or zero magnetic shear breaks up the toroidal coupling and the associated semi-global mode structure, leading to a "discontinuity" (or "gap") between the turbulence inside and outside the q-minimum (q-min) surface. Such a discontinuity prevents particle motion across the q-min surface, suggesting an existence of a transport barrier. The discontinuity effectively works as a transport barrier when the q-min surface is locatedd just outside the maximum pressure gradient. This is consistent with recent JT-60U experimental results. It is also found that plasma shear rotation enhances the character of the discontinuity when the flow direction is in the same direction as the the mode rotation. This significantly suppresses the mode activity near the q-min surface·

Reference

[1-1] Y.Kishimoto, et. al. Phys. Plasmas 3, (1996) 1289.
[1-2] Y.Kishimoto et. al., 16th IAEA Fusion Energy Conf., Montreal, IAEA-CN-64 / DP-10.

2. Stability

Dynamics and acceleration mechanisms of vertical displacement events (VDEs) of elongated

tokamaks are investigated using the Tokamak Simulation Code. It was shown that disruption events, such as a sudden plasma pressure drop (β_p collapse) and the subsequent plasma current quench (I_p quench), can accelerate VDEs due to the adverse destabilizing effect of the resistive shell [2-1]. The essential mechanism of the VDE acceleration was clarified to be the intense enhancement of positional instability due to a large and sudden degradation of the magnetic field decay *n*-index. Additionally, in a tokamak with an up/down asymmetric shell with respect to the geometric midplane, the I_p quench also causes an additional VDE acceleration due to the vertical imbalance of the attractive force.

An amelioration of I_p quench-induced VDEs was experimentally established in JT-60U tokamak by optimizing the plasma vertical location (the neutral point) just prior to the disruption. The JT-60U vacuum vessel is shown to be suitable for preventing the β_p collapse-induced VDE. The neutral point of the ITER-EDA tokamak is found to lie at ~ 22 cm below the plasma magnetic axis of the nominal equilibrium [2-2]. Consequently, it was clarified that the ITER tokamak has an advantage of avoiding the fatal damage of the complicated structures of the bottom-divertor.

In recent experiments of JT-60U, the high performance plasmas have been obtained by the negative shear discharges. In most of such discharges, the β_p -collapse occurs following MHD activities with the fast growth rate of about $100\mu s$ and limits the maximum attainable β -value. It is important to clarify the feature of the ideal MHD stability and to achieve higher plasma performance. Figure 2-1 shows the n=1 toroidal mode stability limit against β_n and $q_{\min}$ for the JT-60U like plasma, where the pressure profile has the steep gradient just inside the radial position of $q_{\min}$. An area above the solid line is unstable. A feature of the stability limit is that when $q_{\min}$ is just below a rational surface, the stability limit becomes lower.

The effects of the q-profile and the pressure profile on the stability limit are investigated. In both profiles on inside and outside regions of $q_{\min}$, the stronger magnetic shear makes β -limit higher, and the stronger pressure gradient has lower β -limit. These show the way to get the higher performance plasma. [2-3]

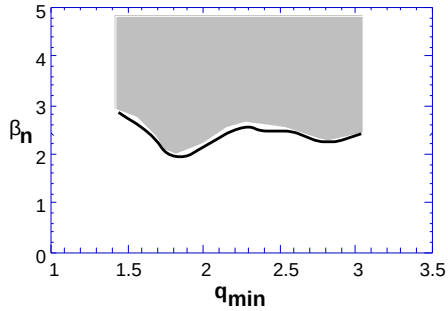

Fig.2-1 Ideal stability of n=1 mode

High energy particles produced by the nuclear fusion reaction or RF heating system resonance with a plasma wave. Among various waves which have the possibility to be excited, Toroidicity-induced Alfven Eigenmode (TAE mode) is considered to be the most important, because the velocity of the high energy particle is close to the Alfven speed. In the JT-60U experiment, the TAE mode in the negative shear plasma is rather stable than that in the positive shear plasma. A theoretical analysis for the TAE mode in the negative shear plasma shows that a large density gradient produced in the internal transport barrier makes the width of the gap of the

shear Alfven continuum spectrum narrower. Therefore, the TAE mode can not exist near the plasma center where the population of high energy particles is high, so that the TAE mode is stabilized[2-4].

The nature of the kinetic ballooning mode in the MHD second stability regime has been clarified through the behavior of the eigenfunction. It has been found to be a continuation of the MHD ballooning mode, not of the second mode with a smaller growth rate which coexists with the MHD mode. The kinetic shooting code has also been applied to the parameters of TFTR in which the kinetic ballooning mode was recently observed. The toroidal mode number and the frequency for the fastest growing mode have been found to be consistent with the experimental observations. Finite beta stabilization of the electrostatic ITG mode and destabilization of the ITG-driven ballooning mode have been demonstrated. The mode stability in the negative shear region, where the MHD ballooning mode is known to be stable, has also been studied. The kinetic ballooning mode persists for $s < 0$ with a narrow stable window near null shear [2-5].

A theory and a numerical method are presented for the asymptotic matching analysis of resistive MHD stability in a negative magnetic shear configuration with two rational surfaces. The theory formulates the problem of solving both the Newcomb equations in the ideal MHD regions and the inner-layer equations around rational surfaces as boundary value/eigenvalue problems to which the finite element method and the finite difference method can be applied. Hence, the problem of the stability analysis can be solved by a numerically stable method. The present numerical method has been applied to model equations having analytic solutions in a negative magnetic shear configuration. Comparison of the numerical solutions with the analytical ones verifies the validity of the numerical method proposed.

References

[2-1] Nakamura Y., Yoshino R., Pomphrey N., et al., “Acceleration Mechanism of Vertical Displacement Event and its Amelioration in Tokamak Disruptions”, J. Nucl. Sci. Technol. **33**, No.8 (1996) 609.

[2-2] Nakamura Y., Nishio S., Yoshino R., et al., J. Plasma & Fusion Res. **72**, No.12 (1996) 1387.

[2-3] shii Y., Ozeki T., Tokuda S., and Takeji S., JAERI-Research 97-047, Section 2.5.

[2-4] Ozeki T., Azumi M., Ishii Y., et al., Plasma Phys. Control. Fusion 39 A371 (1997).

[2-5] Yamagiwa M., Hirose A., and Elia M., "Kinetic shooting code study of ballooning modes in a tokamak", Plasma Phys. Control. Fusion 39 531 (1997).

3. Divertor

A simple five-point model of the scrape-off layer (SOL) plasma outside the separatrix of a diverted tokamak has been developed to study the inside/outside divertor asymmetry [3-1]. The SOL current, gas pumping/puffing in the divertor region, and divertor plate biasing are included in this model. Gas pumping/puffing and biasing are shown to control divertor asymmetry. In addition, the SOL current is found to form asymmetric solutions without external controls of gas pumping/puffing and biasing.

A new "implicit" Monte Carlo (IMC) method has been developed to simulate ionization and recombination processes of impurity ions in divertor plasmas [3-2]. The IMC method takes into account many ionization and recombination processes during a time step Dt . The time step is not limited by a condition, $Dt << t_{min}$ (t_{min}; the minimum characteristic time of atomic processes), which is forced to be adopted in conventional Monte Carlo methods. We incorporate this method into a one-dimensional impurity transport model. In this transport calculation, impurity ions are followed with the time step about 10 times larger than that used in the conventional methods.

References

[3-1] N. Hayashi, T. Takizuka, A. Hatayama, M. Ogasawara, "Analysis of Divertor Asymmetry Using a Simple Five- point Model", JAERI-Research 97-018 (1997).

[3-2] A. Suzuki, T. Takizuka, K. Shimizu, et. al., "An Implicit Monte Carlo Method for Simulation of Impurity Transport in Divertor Plasma", J. Comput. Phys. **131** (1997) 193.

4. Burning

Helium ash removal is an important issue for determining the cost and viability of a fusion reactor based on the magnetically confiment scheme. The ash confinement time is dominated by the edge pumping rate rather than core transport. If helium ash is effectively exhausted in a peripheral region, the helium ash in the central region can be easily removed. A new method for helium ash removal is numerically confirmed by an Orbit Following Monte-Carlo simulation. The key point of the method is preferential coupling of an ICRF wave with He^+ ions without resonance with D^+ and T^+, where He^+ ions are produced by charge-exchange recombination with fuel neutrals near the peripheral region. He^+ ions are driven into the ripple trapped region of velocity space by the ICRF wave. The ripple trapped helium ions are then removed and transported to a pumping duct due to the grad-B drift motion. Numerical results[4-1] show that to reduce helium ash to about half of that without active ash removal and to keep a fusion output of 1.5GW in a reactor-grade tokamak, the required ICRF power is 10~15MW, when the ripple field is greater than 1.5%. In this scenario, it is enough to have an ICRF antenna array and a pumping duct between a pair of toroidal field coils.

References

[4-1] K.Hamamatsu, C.S.Chang et.al., IAEA-CN-64/DP-22 (Proc. 16th IAEA Fusion energy Conf.,Montreal, 1996).

5. Numerical Experiment of Tokamak (NEXT)

5.1 Gyrokinetic/Gyrofluid Model

A self-consistent particle-fluid hybrid simulation model has been formulated based on the nonlinear gyrokinetics in which the electron inertia effect is retained[5-1]. It has been shown that the present hybrid model possess an exact energy invariance. We can afford to use the time step in

the hybrid simulation determined solely by the mode frequency of interest.

A three dimensional gyro-fluid code has also been developed which employs a two field model including the electron kinetic effects. The m = 1 kinetic internal kink instability is simulated by the code. The results from the gyro-fluid simulation agree well with those from the gyrokinetic particle simulation for the linear and early nonlinear stages of the instability[5-2].

5.2 Divertor Simulation

Simulation codes play an essential role in understanding of physical processes in the divertor plasma where the plasma transport, the neutral transport and the impurity transport are strongly coupled with each other. Three representative codes with different purposes are presented [5-3]. A particle code, PARASOL, is being developed to verify the physical model used in fluid codes, such as sheath condition and the heat diffusivity. A fluid code, SOLDOR, is now under development to simulate the divertor plasma accounting for interactions with the neutral particles. A Monte-Carlo code, IMPMC, has been developed for the analysis of the impurity behavior in the divertor plasma. The optimization of these codes for massive parallel computers has just been started.

5.3 Massively Parallel Computing

The kinetic ballooning shooting code, KBSHOOT, developed at the Plasma Physics Laboratory, University of Saskatchewan, Canada, has been parallelized for running on the VPP500 machine. The CPU time has been reduced by a factor of three for the 4PE (Processing Element) mode and by a factor of eight for the 16PE mode, as compared to that of the original code with the 1PE mode[5-4].

Regarding the multiple-nodes simulation of the 1-D electrostatic PIC code, a test particle orbit separates from the orbit in the single-node simulation even for the exactly same stating conditions. Measuring the maximum Lyapunov exponent shows that the separation of particle orbits is not caused by accumulation of numerical errors but caused by the origin of chaos. Therefore, both results from different number of nodes are viewed as realization of an ensemble and equally reliable[5-5].

5.4 Interdisciplinary Research

The physics of disk-star system is clarified through MHD simulations[5-6]. The dipolar magnetic field of the protostar threads the protostellar disk in simulation. A current sheet inside the expanding magnetic loops gives rise to the magnetic reconnection followed by the generation of hot plasmoids. The plasma temperature rises sufficiently to emit hard X-rays to be observed by X-ray satellites such as ASCA. The simulation successfully explained the mass outflow phenomena in protostar as well as X-ray emission.

Generalized magnetic coordinates are constructed from a framework of quadratic flux minimizing surfaces. The coordinates smoothly reduce to straight field line coordinates where flux surfaces exist. A feature of the construction of such surfaces is an efficient identification of the size and phase of magnetic islands, and thus a new technique is enabled by which magnetic islands in the vacuum field of heliacs may be controlled[5-7]. The algorithm for constructing the coordinates is robust and flexible, and requires less field line tracing than present straight field line mapping routines.

References

[5-1] Tokuda S., Naitou H., Lee W. W, "A Particle-Fluid Hybrid Simulation Model Based on Nonlinear Gyrokinetics, " submitted to J. Plasma and Fusion Research.

[5-2] Naitou H., Kitagawa H., Tokuda S., “Linear and Nonlinear Simulation of Kinetic Internal Kink Modes, ” J. Plasma and Fusion Research 73, 174 (1997).

[5-3] K. Shimizu, T. Takizuka, "Simulation of Divertor Plasma", J. Plasma and Fusion Research **72** (1996) 909.

[5-4] Yamagiwa M., Nemoto T., Hirose A., Elia M., "Parallelization of kinetic ballooning shootingcode KBSHOOT, " to be published in JAERI-Data/Code 97-032.

[5-5] Idomura Y., Tokuda S., Wakatani M., “Chaotic behavior in PIC simulation and its relation to computational errors, ” to be published in Comput. Phys. Commun. 102 (1997).

[5-6] Hayashi M., Shibata K., Matsumoto R., “X-ray flares and mass outflows driven bymagnetic interaction between a protostar and surrounding disk, ” Astrophys. J. 468, 37 (1996).

[5-7] S.R. Hudson and R.L. Dewar, “Manipulation of islands in a helical vacuum field, ” Phyics Letters A 226, 85 (1997).

VII. FUSION INTERNATIONAL COOPERATIONS

In the area of fusion research and development, Japan is recognized as one of the leading nations of the world together with Europe, USA and Russian Federation. Fusion reactor development is a long-term project which requires large resources both in man-power and development fund. It covers also broad area of science and technology. International cooperation has been recognized quite efficient in reducing risk as well as in avoiding unnecessary duplication, and in enhancing world's fusion program. JAERI is carrying out various international cooperation in fusion such as the ITER Engineering Design Activity (EDA) under IAEA, the three large tokamak cooperation under IEA, and broad activities under the US-Japan cooperation

International cooperations in terms of fusion research and development are implemented through multilateral cooperations under IEA in Organization for Economics Cooperation and Development (OECD) and IAEA and bilateral cooperations such as Japan-US cooperation. The multilateral and bilateral cooperations carried out in JAERI are summarized in Table VII.1-1 and Table VII.2-1.

1. Multilateral Cooperations

1.1 IAEA

Under the coodination of International Fusion Research Council, International Atomic Energy Agency (IAEA) holds various conferences such as the International Fusion Energy Conference (so called IAEA international conference) and supports the ITER program. The IAEA international conference, which is held every other year, is one of the largest conferences in the area of fusion research. The 17th IAEA international conference is planned to take place in Yokohama, October 1998. IAEA also undertakes the EDA in the ITER program.

1.2 IEA Cooperation

Fusion Power Coordinating Committee (FPCC), which is organized under IEA, coordinates the research and development programs for member nations, selects the important areas and reviews the cooperation activities. Five cooperations are presently carried out in JAERI as shown in Table 1.

The IEA three large tokamak cooperation pursues personal exchange, holding expert meetings and information exchange among JT-60 in Japan, JET in EU and TFTR in USA. Currently six task proposals, namely "High-β_p plasma Research", "Disruption Studies", "Divertor Plate Technology", "Neutral Beam Current Drive Research", "Remote Participation in Experiments" and "Impurity Content of Radiative Discharges", have been successfully continued. Under these tasks, exchanges of personnel, data and discussions have been intensively carried out. For example, under "Remote Participation in Experiments" the effectiveness of remote participation was successfully demonstrated. By using Data Link System and a video conference

system, participants from both JAERI and PPPL jointly analyzed and discussed the JT-60U high performance reversed shear experiments data and achieved a high fusion performance (also described in 1.7.2).

In the Implementing Agreement on Plasma Wall Interaction in TEXTOR, a plasma-wall interaction research cooperation is carried out utilizing the facility of the TEXTOR tokamak built in Forschungszentrum Jülich, Germany.

The agreement for cooperation on fusion materials research is to investigate the irradiation damages by applying neutrons from a fission reactor to fusion materials. In order to develop fusion materials after a prototype reactor, a conceptual design of a 14 MeV intense neutron source (Fusion Materials and Irradiation Test Facility : IFMIF) is carried out by four parties of Japan, USA, EU and Russia.

The agreement for cooperation on environments, safety and economics is to carry out their evaluation researches which are ongoing with particular emphasis upon environments and safety.

The agreement for cooperation on fusion reactor engineering is to carry out research cooperation and information exchange in terms of neutron engineering, tritium breeding blanket, plasma-type volume production neutron source and so on.

Multilateral Cooperation	
IAEA	• ITER (International Thermonuclear Experimental Reactor) /EDA Project [Japan, USA, EC, Russia] • Information Exhange on Large Tokamaks • Information Exchange on Atomic and Molecular Data • International Conferences
IEA	• Three Large Tokamak Cooperation [JT-60(J), TFTR(US), JET(EU)] • Plasma Wall Surface Interaction Program [Japan, USA, EU. Canada] • Programme of Research and Development on Radiation Damage in Fusion Reactor Materials [Japan, EU, Canada, Switzerland, USA] • Joint Program for Environmental, Safety and Economic Performance of Nuclear Fusion Technology [Japan, USA, EU, Canada] • Cooperative Program on Nuclear Technology of Fusion Reactors [Japan, USA, EU, Canada]

Table VII.1-1. Multilateral cooperations in fusion international cooperations at JAERI

2. Bilateral Cooperation

On Japan-US cooperation, Coordinating Committee of Fusion Energy (CCFE) is formed to synthetically coordinate the cooperation activities under Agreement between the government of Japan and the government of the United States on cooperation in Research and Development in Energy and Related Fields. The Japan-US cooperation consists of four frameworks of exchange program, joint program, joint project and plasma physics. In particular, broad joint projects based on agreements and annexes have produced fruit results, playing a leading role in world's fusion research and development.

On Japan-EU cooperation, Agreement for Cooperation between the government of Japan and the European Atomic Energy Community in the field of controlled thermonuclear fusion was concluded February 1988. Based on this agreement, a joint experiment is carried out in which lower hybrid (LH) wave launcher module built at JAERI are installed into the LH test facility in Cadarache Institute.

With Canada, JAERI carries out expert meeting and information exchange on tritium technology and tokamak research through Atomic Energy Canada Ltd. (AECL). With Australia, information exchange and expert exchange are carried out by holding workshops mainly in the area of diagnostics, experiment and theory for toroidal plasmas. With Russia, information exchange and expert meeting on plasma and fusion are planned under Agreement between the government of Japan and the government of Russia in Research and Development in Science and Technology.

Bilateral Cooperation	
Japan - US	• Doublet III Project • HFIR Joint Irradiation Experiment Program • Fusion Fuel Processing Technology Development Program • Cooperation in Fusion Research and Development • Data Link Program • Joint Experiment Program on Negative Ions
Japan - EU	• Cooperative Activities Concerning a Lower Hybrid Antenna Module
Japan -Canada	• Cooperation in the Field of Controlled Nuclear Fusion • Cooperation on the Chronic Tritium Release Experiment
Japan - Australia	• Cooperation on Diagnostics, Experiments and Theory
Japan - Russia	• Cooperation in Fusion Research and Development

Table VII.2-1. Bilateral Cooperations in fusion international cooperations at JAERI

3. Cooperative Program on DIII-D (Doublet III) Experiment

The primary goal of the DIII-D tokamak research program is to provide data for development of a conceptual physics for a commercially attractive fusion power plant. Specific DIII-D objectives include the steady-state sustainment of plasma current as well as demonstrating techniques for microwave heating, divertor heat removal, ash exhaust and tokamak plasma control. The DIII-D program is addressing these objectives in an integration of high beta and good confinement.

3.1 Highlights of Research Results

3.1.1 Divertor and Boundary Research

The major goals of the Divertor and Boundary Physics studies are the control of impurities, efficient heat removal and understanding a role of the edge plasma that plays in the global energy confinement of the plasma. Partially detached plasmas, which is produced by deuterium puffing, make a long (50 cm), radiating divertor leg with only a 2:1 variation of the emission along the leg, exceeding ITER requirement as shown in Fig. VII.3-1. The aim of the ITER divertor solution is to reduce the peak heat flux at the divertor plate by spreading the heat flux along the divertor channel, but ITER only requires a 6:1 uniform spreading. Preliminary analysis indicates that the length of the radiating zone in Fig. VII.3-1 exceeds substantially the predictions of the standard model, requiring investigation of the role of non-coronal and convective effects. The core plasma confinement in the case of Fig. VII.3-1 was progressively reduced to the L–mode level by the high neutral pressures (reaching 1 mTorr) near the core plasma that resulted from the strong gas flow through to the divertor pump and the inadequate divertor baffling in DIII–D. The full installation of the double null, triangular plasma, Radiative Divertor in DIII–D will provide the baffling need to allow simultaneous high performance core plasmas with low impurity and neutral

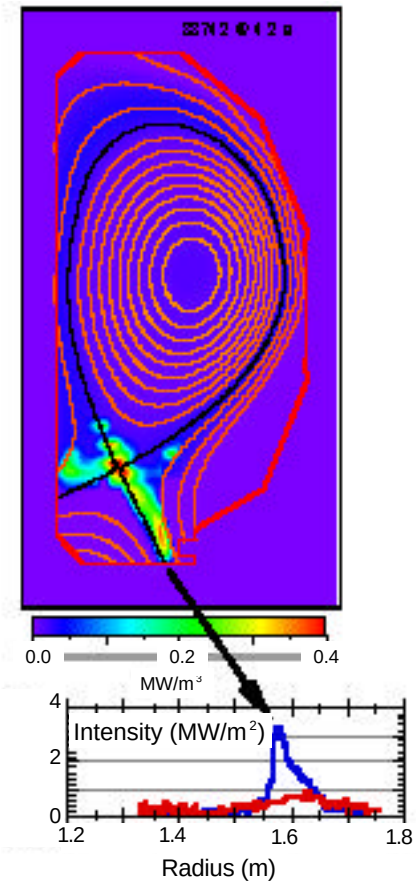

Fig. VII.3-1 Long radiation divertor leg demonstrating effective radiation exceeding ITER requirements

pressure with high plasma and neutral densities in the detached divertor.

3.1.2 Advanced Tokamak Research

The goal of the Advanced Tokamak program is to optimize both energy confinement time and beta in a non inductively driven discharge relevant to steady state operation. To discuss the normalization constants which permit comparisons with certain standard condition to be made, we use H-factor and β_N. Here, H-factor is a ratio of the energy confinement time with the baseline set by ITER-89P L-mode scaling and $\beta_N=\beta_T/(I/aB)$ (%, MA, m, T). The approach of DIII-D to the advanced tokamak is to increase the stability limit of these high confinement regimes without degrading the confinement. The feasibility of an advanced physics approach to tokamak reactors was demonstrated by discharges with negative central magnetic shear (NCS).

NCS discharges are characterized by a non-monotonic safety factor (q) profile and the existence of internal transport barriers supporting steep gradients in T_i, n_e, V_f. L–mode and H–mode NCS discharges with inside limiter, single-null divertor (SND), and double-null divertor (DND) configurations have been produced in DIII–D. A way of combining the favorable feature of enhanced fusion yield in an NCS L–mode with the higher β limit of NCS H–mode was successfully implemented in DIII–D. This is estimated by the ideal MHD calculation (Fig.VII.3-2). An NCS L–mode is produced initially and its β and core pressure are allowed to increase with further heating up to the point when the β limit is approached. Plasma shape control is then deployed to induce a transition to H–mode. The density profile flattens quickly resulting in a broadened pressure profile which in turn raises the β limit. This technique allows a steeper core pressure profile than standard H–mode and a higher β than NCS L–mode. Since the fusion production rate depends on optimizing the pressure profile, this path led to the highest neutron rate on DIII–D to date ($Q_{DT}^{eq}=0.32$).

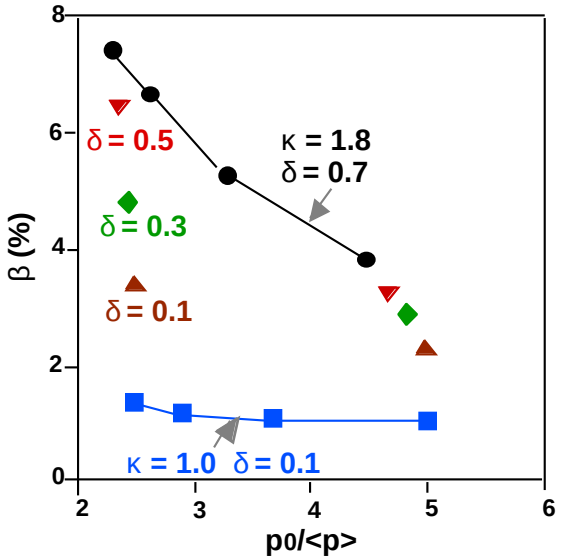

Fig.VII.3-2 Maximum b stable to the ideal n=1 kink mode vs. pressure peaking factor.Results are shown for a circular cross section (k=1) and an elongatied cross section (k=1.8) with various triangularity (d=0.1-0.7).

3.1.3 Tokamak Physics Studies

The Tokamak Physics Program in DIII-D contributes to the fundamental understanding of key physics issues in toroidal confinement system. Understanding what determines the input power threshold for transport barrier formation is important for projection to future tokamaks. Theory has suggested that the threshold is given by the balance between the microinstability growth rate and the ExB shear damping rate, and the internal transport barrier should first form in the plasma core where the magnetic shear stabilization has the biggest impact. This is corroborated by DIII-D measurements which show the core transport barrier first formed in the interior and expanded with increased beam power and contracted with decreased power. The threshold power varies over a wide range in present experiments. DIII–D requires only a few MW to produce the transition to high confinement with internal transport barriers while other tokamaks such as TFTR and JT-60U typically require much higher power. This could perhaps be explained by two possible reasons. The first may be related to the different mechanisms which drive the ExB shear flow. The ExB shear damping rate in toroidal geometry is given by

$$\omega_{ExB} = (B_\theta R/B)\, d(Er/RB_\theta)/dr, \quad 1/(RB_\theta)\, d/dr = d/d\psi,$$

and assuming neoclassical ion poloidal velocity,

$$Er/(RB_\theta) \quad V_\varphi/R + (1-K1)/(Z_i e)\, dT_i/d\psi \quad + T_i/(Z_i e n_i)\, dn_i/d\psi.$$

Since $K1 \sim 1$ in the plasma core, only toroidal flow and density gradient contribute significantly to producing the ExB flow. DIII–D with tangential NBI can induce turbulence suppression effectively with toroidal flow shear from the toroidal momentum input. This is absent for balanced beam injection in which case the flow is purely diamagnetic and the flow drive depends largely on the density gradient. High beam power may thus be required to provide a steep density gradient to drive the flow. The second speculation is that the turbulence growth rate and thus the threshold depends strongly on shape in addition to magnetic shear. This is supported by the H–mode power threshold observed in the DIII–D elongation-ramp experiment and is also consistent with a recent experiment to study bean and peapod configurations on DIII–D. Preliminary results from this experiment indicate that these configurations produce transitions to higher confinement modes readily at low input power. The power threshold to enter an enhanced confinement regime is clearly a subject which needs further study if these enhanced confinement modes are to be applied to next step experiments.

4. Other Activities

The mutual inforamtion and personal exchanges between JAERI and fusion research institutes in Asian area are rapidly increasing during this several years under significant development on fusion research in this area, especially in China and Korea. These exchanges are performed under STA scientist exchange program (in 1998, four scientists from China for one year and two JAERI scientists to China for two weeks), the scientist invitation program (in 1998, one senior scientis from China for one month), STA and JAERI fellowships and so on. A new framework to make more fruitful cooperation between JAERI and these countries on fusion research filed should be prepared under Science and Technology Cooperation Agreement between Japan and these countries.

APPENDICES

A. 1. Publication List (April 1996 - March 1997)

A. 1. 1. List of JAERI reports

1) Aoyagi T., Nagashima K., Kitai T., et al., "The Design Study of the JT-60SU Device -The Power Supply for Coils of JT-60SU-" JAERI-Research 97-010 (1997) (In Japanese).
2) Arai T., Koike T., Shimizu M., JAERI-Tech, 97-003, "Development of Fiber Scope for JT-60 Toroidal Field Coil Cooling Pipe" (1997).
3) Hatano T., Sato K., Fukaya K. et al., "High Heat Flux Testing of HIP Bonded DS-Cu/316SS First Wall Panel for Fusion Experimental Reactors," JAERI-Research 97-017 (1997).
4) Hayashi N., Takizuka T., Hatayama A., et al., "Analysis of Divertor Asymmetry Using a Simple Five-point Model", JAERI-Research 97-018 (1997).
5) Hayashi T., Miya N., Kikuchi M., et al., "The Design Study of the JT-60SU Device (No.9) -Fuel Handling, Confinement and Clean up Systems for JT-60SU-" JAERI-Research 97-007 (1997) (In Japanese).
6) Ishida S., "Review of JT-60U Experimental Results from February to November, 1996" JAERI-Research 97-047 (1997) (in Japanese).
7) Ishii Y., Ozeki T., Tokuda S., et al., "Review of JT-60U Experimental Results from February to November 1996", JAERI-Research 97-047, Section 2.5.
8) Kawai M.,etc,"Development of the Negative-ion Based NBI Computer System for the JT-60", JAERI-Tech 97-012,P.69.
9) Kikuchi M., Nagami M., Kurita G., et al., "The Design Study of The JT-60SU Device (vol.1) -Objectives and Outline of JT-60SU Program-" JAERI-Research 97-026 (1997) (in Japanese).
10) Kikuchi M., "An Economical Consideration of Fusion Reactor Advanced SSTR (A-SSTR)" JAERI-Research 97-004 (1997) (In Japanese).
11) Kurita G., Nagashima K., Tobita K., et al., "The Design Study of The JT-60SU Device -The Physical Design and Diagnostic System of JT-60SU-" JAERI-Research 97-023 (1997) (in Japanese).
12) Kuriyama M., Ushigusa K., Ito T., et al., "The Design Study of the JT-60SU Device-The Neutral Beam Injection System of JT-60SU-" JAERI-Research 97-005 (1997) (In Japanese).
13) Liu C.G., Yamagiwa M., Qian S.J., "Production of sheared flow by means of ICRF heating in tokamak plasmas", JAERI-Research 96-068 (1997).
14) Maebara S., Seki M., Suganuma K. et al., "Development of a new lower hybrid antenna module using a poloidal power divider" JAERI-Research 96-036 (1996).
15) Nakamura Y., Yoshino R., Pomphrey N., et al., "Extremely Fast Vertical Displacement Event Induced by a Plasma bp Collapse in High bp Tokamak Disruptions," JAERI-Research 96-023 (1996).
16) Neyatani Y., Mori K., Oguri S., et al.,"Magnetic Sensor for Steady State Tokamak" JAERI-Research 96-026 (1997) (in Japanese).
17) Neyatani Y., Ushigusa K., Tobita K., et al., "The Design Study of The JT-60SU Device -The vacuum vessel and cryostat of JT-60SU" JAERI-Research 97-024 (1997) (in Japanese).
18) Nishitani T., Iguchi T., Ebisawa K., et al, "Design of Radial Neutron Spectrometer for ITER", JAERI -Tech 96-038(1996)
19) Nishitani T., Iida T., Ikeda Y., et al., "Irradiation Tests on Diagnostics Components for ITER in 1995", JAERI-Tech 96-040(1996)
20) Sato M., Isei N., Isayama A., et al., "Determination of Radial Position in the Measurement of Electron Temperature Profiles from Electron Cyclotron Emission", JAERI-Research 97-011 (1997).
21) Seki M., Obara K., Maebara S. et al., "Performance test of lower hybrid waveguide under long/high-RF power transmission" JAERI-Research 96-025 (1996).
22) Tokamak Program Division (Compiled by Toyosima N.), "Material Characteristic of Ti Alloy (Ti-6Al-4V)" JAERI-Research 97-012 (1997) (in Japanese).
23) Tokuda S., Watanabe T., "Finite Difference Method for Inner-layer Equations in the Resistive Magnetohydrodynamic Stability Analysis," JAERI-Research 96-004 (1996).

24) Tokuda S., Watanabe T., "Theory of Asymptotic Matching for Resistive Magnetohydrodynamic Stability in a Negative Magnetic Shear Configuration," JAERI-Research 96-057 (1996).
25) Toyoshima N., Masaki K., Kaminaga A., et al., "The Design Study of the JT-60SU Device - Auxiliary System, Plan of Displacement, and Dismantlement Construction-" JAERI - Research, 97-008, 148 (1997) (In Japanese).
26) Ushigusa K., Mori K., Nakagawa S., et al., "The Design Study of The JT-60SU Device -The Superconductor-Coils of JT-60SU-" JAERI-Research 97-027 (1997) (in Japanese).
27) Yamamoto T., Ushigusa K., Sakamoto K., et al., "The Design Study of the JT-60SU Device -The ECRF System of JT-60SU-" JAERI-Research 97-006(1997) (In Japanese).
28) Yoshida H., Naito O., Hatae T., et al., "Solution for a window coating problem developed in the JT-60U Thomson scattering system", JAERI -Research 96-062(1996)
29) Yoshida H., Naito O., Yamashita O., et al., "JT-60U Thomson scattering system with multiple ruby lasers and high spatial resolution for high electron temperature plasma measurement", JAERI-Research 96-061(1996)

A. 1. 2. List of papers published in journals

1) Aoyagi T., "Examples of Data Processing Systems / Data Processing System for JT-60", J. Plasma and Fusion Research 72 (1996) 1370-1375.
2) Asakura N., Hosogane N., Iio S., et al., "Field Reversal Effects on Divertor Plasmas under Radiative and Detached Conditions in JT-60U", Nucl. Fusion, 36, 795 (1996).
3) Cordey J.G., Takizuka T., Miura Y., et al., "ITER Forecasts", Science 275 (1997) 290-291.
4) Fujita T., Ide S., Shirai H., et al., "Internal Transport Barrier foe Electrons in JT-60U Reversed Shear Discharges", Phys. Rev. Lett. 78, 2377 (1997).
5) Hoek M., Nishitani T., Carlson M., et al., "Triton burnup measurements by neutron activation at JT-60U ", Nucl. Instrum. Methods A368(1996) 804-814
6) Horton W., Tajima T., Kishimoto Y., et al., "Ion transport analysis of a high-beta poloidal JT-60U discharge", Plasma Phys. Control. Fusion 38 (1996) 1323-1326.
7) Horton W., Tajima T., Kishimoto Y., et al., "Thermal Transport Barriers in Tokamaks from Bifurcations in the Sheared Mass Flows", Comments Plasma Phys. Controlled Fusion 17 (1996) 205-219.
8) Hudson S.R. and Dewa R.L., "Almost invariant surface for magnetic field-line flows," Journal of Plasma Physics, 56(2):361, 1996.
9) Hudson S.R. and Dewa R.L., "Manipulation of islands in a heliac vacuum field," Physics Letters A, 226:85,1997.
10) Ide S., Fujita T., Naito O., et al., "Sustainment and Modification of Reversed Magnetic Shear by LHCD on JT-60U", Plasma Physics and Controlled Fusion, 38 1645 (1996).
11) Ide S., Naito O., Kondoh T., et al., "Response of Lower Hybrid Wave Driver Current profile on Wave Launching Position", Nucl. Fusion, 36, 1057 (1996).
12) Ikeda Y. Tobita K. Hamamatsu K., et al , "Ripple Enhanced Banana Drift Loss at the Outboard Wall during ICRF/NBI Heating in JT-60U ", Nuclear Fusion 36 759-767 (1996).
13) Ishida T., Hayashi T., Yamada M. et al., "R&D of a Compact Detritiation System Using a Gas Separation Membrane Module" Fusion Technol., 30,926-930 (1996).
14) Itami K., Yoshino R., Asakura N.,et al., "Isolation of the improved core confinement from high recycling and radiative boundary in reversed magnetic shear plasmas of JT-60U", Phys. Rev. Lett. 78, 1267 (1997).
15) Itoh Y., Ogiwara N., Saidoh M., et al., "Simulation of RBS spectra for a surface with a periodic roughness", Nucl. Instrum. Methods, B117, 161-169, (1996).
16) Jimbou R., Saidoh M., Nakamura K. et al., "New composite composed of boron carbide and carbon fiber with high thermal conductivity for first wall," J. Nucl. Materials, 233-237, 781-786 (1996).
17) Kawano Y., Nagashima A., Hatae T., et al., "Dual CO2 Laser interferometer with a wavelength combination of 10.6 and 9.27 mm for electron density measurement on large tokamaks", Rev.Sci.Instrum. 67(1996) 1520

18) Kikuchi. M. and JT-60 team., "Recent Results of JT-60U"(invited), Fusion Technology, 30, No.3, Part2A 660 (1996).
19) Kikuchi. M., "An Economically Competitive Fusion Reactor" (invited), Fusion Technology, 30, No.3, Part2B 1631 (1996).
20) Kimura H. and JT-60 Team, "Recent results from high performance and steady state researches in the Japan Atomic Energy Research Institute Tokamak 60 Upgrade", Physics of Plasmas, 3, 1943 (1996).
21) Kishimoto Y., "3-Dimensional Simulation Model of Raman Regime Free-Electron Laser", J. Phys. Soc. Jpn. 65 (1996) 3877-3889.
22) Kishimoto Y., Tajima T., Horton W., et al., "Theory of Self-organized Critical Transport in Tokamak Plasmas", Phys. Plasmas 3 (1996) 1289-1307.
23) Kuriyama M., et al, "Development of Negative-Ion Based NBI System for JT-60(in Japanese)", Journal of the Atomic Energy Society of Japan (8.11.30) VOL.38 NO.11 P.912.
24) Kuriyama M., et al, "Trend of High Power Negative-Ion Based NBI Development (in Japanese)", Journal of Plasma and Fusion Research VOL.72 NO.11 P.1162
25) Masaki K., Kodama K., Ando T., et al., "Tritium retention in graphite inner wall of JT-60U", Fusion Engineering & Design 31, 181-187 (1996).
26) Matsuda T., "Data Utilization", J. Plasma and Fusion Research 72 (1996) 1235-1242.
27) Miura Y. and JFT-2M Group, "Change of neutral energy distribution at L/H, H/L transitions and ELMs in the JFT-2M tokamak", Nucl. Fusion, 37, 175 (1997).
28) Miura Y., Okano F., Suzuki N., et al., "Ion Heat Pulse after Sawtooth Crash in the JFT-2M Tokamak", Phys. Plasmas 3, 3696-3700 (1996).
29) Nagashima K., Ide S., Naito O., "Particle Transport Analysis in Lower Hybrid Current Drive Discharges of JT-60U", Plasma Physics and Controlled Fusion, 38, 1975-1984 (1996).
30) Naito O., Yoshida H., Hatae K., et al., "A formula for reconstructing fully relativistic electron distribution from in coherent Thomson scattering data", Physics of Plasmas, 4, 1171-1172 (1997).
31) Naitou H., Kitagawa H., Tokuda S., "Linear and Nonlinear Simulation of Kinetic Internal Kink Modes", J. Plasma and Fusion Research 73, 174 (1997)
32) Nakamura Y., Yoshino R., Neyatani Y., et al., "Mechanism of Vertical Displacement Events in JT-60U Disruptive Discharges," Nucl. Fusion 36 (1996) 643.
33) Nakamura Y., Yoshino R., Pomphrey N., et al., "Acceleration Mechanism of Vertical Displacement Event and its Amelioration in Tokamak Disruptions", J. Nucl. Science & Technol. 33 (1996) 609.
34) Neudatchin S.V., Takizuka T., Shirai H., et al., "Time Behavior of Heat Diffusivity during L-H-L Transition in JT-60U", Jpn. J. Appl. Phys. 35 (1996) 3595-3602.
35) Nishitani T., Hoek M., Harano H., et al., "Triton burnup study in JT-60U ", Plasma Phys. Control. Fusion, 38(1996) 355-364
36) Ogiwara N., Miyo Y., Ueda Y., "Application of the time-of-flight measurements in XHV by a quadrupole mass spectrometer", Vacuum, 47, 575 (1996).
37) Ozeki T., Azumi M., Ishii Y., et al., "Physics issues of high bootstrap current tokamaks", Plasma Phys. Control. Fusion 39 A371 (1997).
38) Qiang Ji, Singer C., Hirayama T., "Simulation of JT-60 Discharges with an Experimentally Calibrated Theoretical Transport Model", Jpn. J. Appl. Phys. 35 (1996) 2797-2802.
39) Ryter F. and H-mode Database Working Group, "Results from the ITER H-mode threshold database", Plasma Phys. Control. Fusion, 38, 1279 (1997).
40) Ryter F., H-mode Database Working Group(Takizuka T., Miura Y., et al.), "H Mode Power Threshold Database for ITER", Nucl. Fusion 36 (1996) 1217-1264.
41) Saigusa M., Moriyama S., Kimura H. et al., "Effect of Non-Linear Wave Absorption on the Radiation Loss Fraction during second Harmonic Minority Heating Experiments in JT-60U," Jpn. J. Appl. Phys., 36, 345-349(1997).
42) Sato M., Fukuda T., Takizuka T., et al., "Threshold power for the H-mode transition in JT-60", Plasma Phys. Control. Fusion, 38, 1283 (1996).
43) Shimizu K., Takizuka T., "Simulation of Divertor Plasma", J. Plasma and Fusion Research 72 (1996) 909-915.
44) Takizuka T., Ogawa Y., Toi K., et al. , "Confinement and Transport / Database and Modelling

Related to ITER", J. Plasma and Fusion Research 72 (1996) 498-504.
45) Ushigusa K., "Simple Modeling to Explain Temperature Dependence of the Lower Hybrid Current Drive Efficiency", Plasma Physics and Controlled Fusion, 38, 1825-1830 (1996)
46) Yamagiwa M., "Positron-emitting radionuclide yield in deuterium beam-injected 3He plasma", Nuclear Science and Engineering 125 218-222 (1997).
47) Yamagiwa M., Hirose A., and Elia M., "Kinetic shooting code study of ballooning modes in a tokamak", Plasma Phys. Control. Fusion 39 531 (1997).
48) Yamauchi T., Grek B., Hoshino K., et al., "Detailed profile of m=2 island with TVTS on JFT-2M", Physics Letters A, 223, 179 (1996).
49) Yamauchi T., Ishige Y., Shiina T., et al., "Development of high-spatial resolution TV Thomson scattering system for JFT-2M", Journal of Plasma and Fusion Research, 72, 692 (1996) (in Japanese).
50) Yoshida H., Naito O., Hatae T., et al., " Approach to a window coating problem by in situ transmission monitoring and laser blow-off cleaning developed in the JT-60U Thomson scattering system", Rev. Sci. Instrum. 68(1) 256-257
51) Yoshida H., Naito O., Matoba T., et al., "Quantitative method for precise, quick, and reliable alignment of collection object fields in the JT-60U Thomson scattering diagnostic", Rev. Sci. Instrum. 68(2) 1152-1161
52) Yoshino R., Koga J.K., Takeda T., "Sensor Algorithms of the Plasma Vertical Position to Avoid a Vertical Displacement Event dusting Plasma-Current Quench on JT-60U", Fusion technology, 30, 237 (1996).
53) Yoshino R., Kondoh T., Neyatani Y., et al., "Fast plasma shutdown by killer pellet injection in JT-60U wit reduced heat flux on the divertor plate and avoiding runaway electron generation", Plasma Phys. Control. Fusion, 39, 313 (1997).
54) Yoshino R., Nakamura Y., Neyatani Y., "Avoidance of VDEs during Plasma Current Quench in JT-60U", Nucl. Fusion, 36, 295 (1996).
55) Yoshino R., Ohsawa M., "Fluctuations in Plasma Equilibrium Control on JT-60U", Fusion Technology, 30, 159 (1996).
56) Yoshino R., Seki M., "Low electric field (0.08Vm-1) plasma-current start-up in JT-60U", Plasma Phys. Control. Fusion, 39, 205 (1997).

A. 1. 3. List of papers published in conference proceedings

1) Arai T., Honda M., Koike T., et al., "Inspection techniques for JT-60 toroidal field coil cooling pipes", 19th SOFT, Lisbon, Portugal, (1996).
2) Asakura N., Koide Y., Itami K., "SOL Plasma Profiles under Radiative and Detached Divertor conditions in JT-60U", 12th Int. Conf. on Plasma Surface Interactions in Controlled Fusion Devices (St. Raphael) (1996).
3) Dacosta O., Kimura H., Moriyama S., et al., "Ion Cyclotron Emission (ICE) New Experimental Results in JT-60U, Theory of Direct Emission", Proc. of Int. Conf. on Plasma Physics, 1, 246 (1996).
4) Hamamatsu K., Nishitani T., Tani K., et al., "Transport and Losses of Energetic Tritons and Beam Ions in JT-60U", IEA Tripartite Workshop on TAE and Energetic Particle Physics, Naka Fusion Research Establishment, JAERI, February 25-27, 1997.
5) Higashijima S., Kubo H., Sugie T., et al., "Study of Carbon Impurity Generation by Chemical Sputtering in JT-60U", 12th Int. Conf. on Plasma Surface Interactions in Controlled Fusion Devices (St. Raphael) (1996).
6) Hiratsuka H., Sasajima T., Kodama K., et al., "Effect of plasma behavior on in-vessel components in JT-60 operation, 19th SOFT, Lisbon, Portugal, (1996).
7) Jimbou R., Kodama K., Saidoh M., et al., "Thermal conductivity and retention characteristics of

composites made of boron carbide and carbon fibers with extremely high thermal conductivity for first wall", 12th Inter. Conf. on Plasma Surface Interactions in Controlled Fusion Devices (1997).
8) Kamada Y., "Characteristics of and issues regarding combined H-mode", Plasma Physics and Controlled Fusion Vol.38, No.8(1996) P.P.1173-1188
9) Kamada Y., Yoshino R., Neyatani Y., et al., "Onset Condition of ELMs in JT-60U", Plasma Phys. Control. Fusion 38 (1996) 1387-1391.
10) Kishimoto Y., Kim J.Y., Azumi M., et al., "Theory and simulation of self-organized critical transport by toroidal ITG turbulence in tokamak plasmas", Theory of Fusion Plasma, Joint Varenna-Lausanne International Workshop, Villa Monastero, Varenna, Italy, August 26-30, 1996.
11) Koide Y. and the JT-60 Team, "Progress in the JT-60U Experiments with Negative- ion Based Neutral Beams", 38th Annual Meeting of American Physical Society, Division of Plasma Physics, Denver, 3IA 2 (1996).
12) Kurihara K. and Kawamata Y., "Development of a Precise Long-time Digital Integrator for Magnetic Measurements in a Tokamak," in Proceedings of 19th Symposium on Fusion Technology, Lisbon, Portugal (1996).
13) Kuriyama M, Akino N, Aoyagi T, et al., "Initial Beam Operation of 500keV Negative-Ion-Based NBI system for JT-60U," Proc. of the 19th Symp. on Fusion Tech., Lisbon (1996).
14) Linke J., Akiba M., Bolt H. et al., "Performance of beryllium, carbon and tungsten under intense thermal fluxes," Proc. 12th Int. Conf. on Plasma Surface Interactions in Controlled Fusion Devices, pp.210, St.Raphael, France, May 20-24 (1996).
15) Maebara S., Seki M., Suganuma K., "Development of a new lower hybrid antenna module using a poloidal power divider," Proc. of 19th Symp. on Fusion Tech. Portugal (1996).
16) Miyamoto K, Akino N, Ebisawa N et al., "Production of Multi-MW Deuterium Negative Ion Beams for Neutral Beam Injectors," Proc. of the 16th IAEA Fusion Energy Conf, Montreal, F1-CN-64/G2-5 (1996).
17) Mori M., "Active Control of H-mode", Plasma Physics and Controlled Fusion Vol.38,No.8(1996) P.P.1189-1200
18) Nakamura Y., Yoshino R., Pomphrey N., et al., "VDE Dynamics and Acceleration / Deceleration Mechanisms in Tokamak Disruptions", American Physical Society, Program of the Thirty-Eighth Annual Meeting of the Division of Plasma Physics, Denver Colorado (1996).
19) Nakamura Y., Yoshino R., Pomphrey N., et al., "βp Collapse-Induced Vertical Displacement Event in High βp Tokamak Disruptions", Plasma Phys. Contr. Fusion 38 (1996)1791-1804.
20) Nishitani T., Iguchi T., Takada E., et al., "Neutron Spectrometers for ITER", Diagnostics for Experimental Thermonuclear Fusion Rector Plenum Press New York(1996)
21) Ogawa H., Kawashima H., Miura Y. and JFT-2M Group, "Closed divertor experiments on JFT-2M", Proceedings of 16th Int. Conf. on Plasma Physics, Nagoya, 1996, 2, 1250 (1997).
22) Ohsawa M., Yoshino R., "Vertical displacement caused by giant ELM in JT-60U", Proc. of Int. Conf. on Plasma Physics, 1, 638 (1996).
23) Ryter F., H-mode Database Working Group(Miura Y., Takizuka T., et al.), "Results from the ITER H-mode Threshold Database", Plasma Phys. Control. Fusion 38 (1996) 1279-1282.
24) Sakurai S., Asakura N., Itami K., "Effect of Particle and Heat Fluxes and Carbon Generation during ELMy Phase in JT-60U", Proc. of Int. Conf. on Plasma Physics, 1, 646 (1996).
25) Sakurai S., Hosogane N., Kodama K., et al., "Design of a Compact W-Shaped Pumped Divertor in JT-60U", 19th. Symp. on Fusion Technology (Lisbon) (1996).
26) Sato M., Fukuda T., Takizuka T., et al., "Threshold Power for the H-mode Transition in JT-60U", Plasma Phys. Control. Fusion 38 (1996) 1283-1288.
27) Sato M., Ishida S., Isei N., et al., "Determination of radial position in the measurement of electron temperature profiles from electron cyclotron emission", Proceedings of 16 th Int. Conf. on Plasma Physics, Nagoya, 1996, 2, 1438 (1997).

28) Sengoku S. and JFT-2M Group, "Coexistent regime of H-mode with a dense & cold divertor plasma in JFT-2M closed divertor", Bull. Am. Phys. Soc. 41, 1487 (1996).
29) Shimizu K., Takizuka T., Sakasai S., "A Review on Impurity Transport in Divertors", 12th Int. Conf. on Plasma Surface Interactions in Controlled Fusion Devices, Saint-Raphael, France, May 20-24, 1996.
30) Shimizu K., Takizuka T., Tokuda S., et al., "Monte Carlo Modeling of Impurity Transport in Divertor Plasma", IAEA Technical Committee Meeting on Advances in Computer Modeling of Fusion Plasmas, Los Angels, 2-4 October, 1996.
31) Shirai H., Takizuka T., Koide Y., et al., "Time Evolution of Transport Properties in JT-60U H-mode Plasmas with Improved Core Confinement", Plasma Phys. Control. Fusion 38 (1996) 1455-1460.
32) Shirai H., Takizuka T., Sato M., et al., "Analyses of Electron and Ion Transport Properties in JT-60U H-mode Plasmas with Improved Core Confinement" Proc. 23rd Eur. Phys. Soc. Conf. on Control. Fusion and Plasma Phys. (1996, Kiev), Vol. 1, page 339
33) Takenaga H., Asakura N., Shimizu K., et al., "Effects of Edge and Central Fueling and particle Confinement in JT-60U", 12th Int. Conf. on Plasma Surface Interactions in Controlled Fusion Devices (St. Raphael) (1996).
34) Takenaga H., Kubo H., Sugie T., et al., "Neutral Deuterium and Helium Behavior in JT-60U Divertor Plasmas", Proc. of Int. Conf. on Plasma Physics, 1, 642 (1996).
35) Takizuka T., "Particle Simulation of Divertor Plasma", Proc. Australia-Japan Workshop on Plasma Theory and Computation, Robertson, Australia, 15-17 November, 1995 (Research School of Physical Science and Engineering, Australian National University, Canberra, 1996) ANU-PRL-TR-96/01, 67-69.
36) Takizuka T., "Scaling Study and Modeling of Improved Confinement", US-Japan JIFT Workshop on Plasma Turbulence and Transport in Toroidal Systems, Kyoto University, 29-31 October, 1996.
37) Tokuda S., Takizuka T., Kishimoto Y., et al., "Massively Parallel Computing with Plasma Simulation Codes in Tokamak Research", Proc. Australia-Japan Workshop on Plasma Theory and Computation, Robertson, Australia, 15-17 November, 1995 (Research School of Physical Science and Engineering, Australian National University, Canberra, 1996) ANU-PRL-TR-96/01, 70-72.
38) Tsuchiya K., Takenaga H., Fukuda T., et al., "Effect of Edge Neutrals on the Condition of the H-mode Transition in JT-60U", Plasma Phys. Control. Fusion 38 (1996) 1295-1299.
39) Watanabe K., Akino N., Aoyagi T. et al., "Recent progress of high power negative ion beam development for fusion plasma heating" The 7th International Symp. on Advanced Nuclear Energy Research, Takasaki, March 18 - 20 (1996).
40) Watanabe K., et al.,"Recent progress of High-Power Negative on Beam Development for Fusion Plasma Heating", 7th Int. Symp. on Advanced Nuclear Energy Research (8.3.22 Takasaki)
41) Yagyu J., Ogiwara N., Saidoh M., et al., "Properties of thin boron coatings formed during deuterated-boronization in JT-60", 12th Inter. Conf. on Plasma Surface Interactions in Controlled Fusion Devices, Saint Raphael, France, (1996).
42) Yamagiwa M., Hirose A., Elia M., "Kinetic analyses of ballooning modes in tokamaks", Proc. 1996 International Conference on Plasma Physics (ICPP, Nagoya, 1996), Vol. 1, 366 (1997).
43) Yamaki T., Gotoh Y., Jimbou R., et al., "Erosion and thermal desorption characteristics of 1D-CF/B4C composite", 12th Inter. Conf. on Plasma Surface Interactions in Controlled Fusion Devices, Saint Raphael, France, (1996).

A. 1. 4. List of other papers

1) Asakura N., Takizuka T., Itami K., "High Density H-mode in JT-60U", 4th Meeting of ITER Confinement Database and Modelling Expert Group, Moscow, 15-17 April, 1996.
2) Fukuyama A., Takizuka T., "Present Status of CDBM Transport Modelling", 4th Meeting of ITER Confinement Database and Modelling Expert Group, Moscow, 15-17 April, 1996.
3) Kamada Y., Takizuka T., JT-60 Team, "Status of JT-60U Experiments and Future Plan", 4th Meeting of ITER Confinement Database and Modelling Expert Group, Moscow, 15-17 April, 1996.
4) Kimura H., "ICRF Heating Results on JT-60U", Meeting of the European Coordinating Committee on Fast Wave Heating and Current Drive (Garching), (1996).
5) Kondoh T., Kimura H., Kusama Y., et al., "Confinement and Loss of MeV-protons in JT-60U ICRF Experiments", IEA Tripartite Workshop on TAE Modes and Energetic particle Physics ,W36 (Naka) (1996).
6) Nagashima A., "Experiment Status of JT-60U/JFT-2M", 4th Japan Australia Diagnostic Workshop (Canberra) (1996).
7) Nagashima A., "Recent Progress of Dual CO2 Interferometer", 4th Japan Australia Diagnostic Workshop (Canberra) (1996).
8) Nakamura Y., Yoshino R., Pomphrey N., et al., "TSC Analyses on VDE Dynamics and Acceleration Mechanism during Disruptions", 4th ITER Physics R&D Expert Group Meeting on Disruption, Plasma Control and MHD, JAERI-Naka, April 15-18, 1996.
9) Neyatani Y., "Hallow Current", Journal of Plasma and Fusion Research Vol.72 No.5 (1996) P.P.403-414
10) Ogawa Y., Hiwatari R., Takizuka T., "Transport Simulation of JT-60U Discharges", 5th Workshop of ITER Confinement Database and Modelling Expert Group, Montreal, 13-16 October, 1996.
11) Saidoh M., "Effect of plasma behavior on tokamak components under JT-60 operation",Tripartite Exchange Agreement Workshop, JET, England, Sept. 10-12, (1996).
12) Sakasai S., "Divertor of JT-60U", Japan US Workshop on High Flux Components and Plasma Surface Interactions for Next Fusion Devices (Naka) (1996).
13) Takizuka T., "Activity Plan for the Task 4.5", 5th Workshop of ITER Confinement Database and Modelling Expert Group, Montreal, 13-16 October, 1996.
14) Tobita K., Fukuyama J., "Physics of a-particles (ITER Physics R&D)", Journal of Plasma and Fusion Research Vol.72 No.6 (1996) P.495
15) Ushigusa K., Fukuyama J., "Heating and Current Drive on ITER", Journal of Plasma and Fusion Research, 72, 517 (1996).
16) Yamagiwa M., Hirose A., Elia M., "Kinetic shooting code study of ballooning modes in tokamak", University of Saskatchewan, Plasma Physics Laboratory Report, PPL-163 (1997).

A.2 Scientific Staffs in the Naka Fusion Research Establishment (April,1996 - March, 1997)

Naka Fusion Research Establishment
- SHIMAMOTO Susumu (Director General)
  - OHKAWA Tihiro (Scientific Consultant)
  - SEKIGUCHI Tadashi (Scientific Consultant)
  - TANAKA Yuji (Scientific Consultant)
  - MIYAMOTO Kenro (Invited Researcher)
  - TANAKA Masatoshi (Invited Researcher)
  - TOMABECHI Ken (Invited Researcher)

Department of Administrative Services
- KOMAKI Akira (Director)
- KUNIEDA Shunsuke (Deputy Director)

Department of Fusion Plasma Research
- KISHIMOTO Hiroshi (Director)
- AZUMI Masafumi (Deputy Director)
- TAKAHASHI Ichiro (Administrative Manager)

Tokamak Program Division
- NAGAMI Masayuki (General Manager)

KIKUCHI Mitsuru	KITAI Tatsuya(*8)	KOIDE Yoshihiko
KURITA Genichi	MORI Katsuharu(*8)	MIYA Naoyuki
NAGASHIMA Keisuke	NAITO Osamu	NAKAGAWA Shouji(*8)
OGURI Shigeru(*8)	TAMAI Hiroshi	TOYOSHIMA Noboru
USHIGUSA Kenkichi		

Plasma Analysis Division
- HIRAYAMA Toshio (General Manager)

HAGINOYA Hirofumi (*16)	HAMAMATSU Kiyotaka	KIM Jin Yong (*18)
KISHIMOTO Yasuaki	NAKAMURA Yukiharu	
NEUDATCHIN SergeiV.(*9)	OHSHIMA Takayuki	POLEVOI Alexei(*5)
SAITO Naoyuki	SAKATA Shinya	SATO Minoru
SHIRAI Hiroshi	TAKIZUKA Tomonori	TSUGITA Tomonori
TSURUOKA Takuya (*14)	WATANABE Kazuhiko (*16)	

Large Tokamak Experiment Division I
- MORI Masahiro (General Manager)

CAO Jianyong(*17)	CHIBA Shinichi	FUKUDA Takeshi
GAO Xiang(*3)	GUNJI Souichi	HARANO Hideki(*21)
ISAYAMA Akihiko	ISEI Nobuyuki	ISHIDA Shinichi
KAMADA Yutaka	KASHIWABARA Tsuneo	KAWANO Yasunori
KAZAMA Daisuke	KITAMURA Shigeru	KOKUSEN Shigeharu
KRAMER Gerrit Jakob(*18)	KUSAMA Yoshinori	MORIOKA Atsuhiko
NAGAYA Susumu	NEMOTO Masahiro	NEYATANI Yuzuru
NISHITANI Takeo	OIKAWA Toshihiro	ONOSE Yoshiaki
SHITOMI Morimasa	SUNAOSHI Hidenori	TAKEJI Satoru
TCHERNYCHEV Fedor Vsevodovich (*4)		TOBITA Kenji
TSUCHIYA Katsuhiko	TSUKAHARA Yoshimitsu	URAMOTO Yasuyuki
YAMASHITA Osamu	YAN Longwen(*17)	YOSHIDA Hidetoshi

Large Tokamak Experiment Division II
YOSHINO Ryuji (General Manager)

ASAKURA Nobuyuki	DaCOSTA Olivier (*1)	
FUJITA Takaaki	HATAE Takaki	HIGASHIJIMA Satoru
HOSOGANE Nobuyuki	IDE Shunsuke	ITAMI Kiyoshi
KIMURA Haruyuki	KONDOH Takashi	KONOSHIMA Shigeru
KUBO Hirotaka	NAGASHIMA Akira	OHSAWA Masaya(*10)
SAKASAI Akira	SAKURAI Shinji	SHIMIZU Katsuhiro
SUGIE Tatsuo	TAKENAGA Hidenobu	

Plasma Theory Laboratory
HIRAYAMA Toshio(Head)

HUDSON Stuart(*18)	ISHII Yasutomo	
KAWANOBE Mitsuru (*14)	MATSUMOTO Taro	OZEKI Takahisa
TOKUDA Shinji	TUDA Takashi	YAMAGIWA Mitsuru

Experimental Plasma Physics Laboratory
SUZUKI Norio (Head)

HOSHINO Katsumichi	KAWAKAMI Tomohide	KAWASHIMA Hisato
LIU Wandong(*21)	MAEDA Mitsuru(*7)	MAENO Masaki
MIURA Yukitoshi	OGAWA Hiroaki	OGAWA Toshihide
OASA Kazumi	SATO Masayasu	SENGOKU Seio
SHIINA Tomio	UEHARA Kazuya	
YAMAUCHI Toshihiko		

Department of Fusion Facilities
FUNAHASHI Akimasa (Director)
SHIMIZU Masatsugu (Deputy Director)

Fusion Facility Administration Division
TAKAHASHI Ichiro (General Manager)

JT-60 Facility Division I
KIMURA Toyoaki (General Manager)

ADACHI Hironori(*11)	AKASAKA Hiromi	ARAKAWA Kiyotsugu
FUKUDA Hiroyuki(*8)	FURUKAWA Hiroshi(*15)	KAWAMATA Youichi
KURIHARA Kenichi	MATSUKAWA Makoto	MIURA Yushi
NOBUSKA Hiromichi(*15)	OKANO Jun	OMORI Shunzo
OMORI Yoshikazu	OOBA Toshio(*15)	SEIMIYA Munetaka
SHIMONO Mitugu	TAKANO Shoji(*16)	TERAKADO Tsunehisa
TOTSUKA Toshiyuki		

JT-60 Facility Division II
SAIDOH Masahiro (General Manager)

ARAI Takashi	HIRATSUKA Hajime	HONDA Masao
ICHIGE Hisashi	KAMINAGA Atsushi	KODAMA Kozo
KOMURO Ken-ichi(*13)	MASAKI Kei	MIYATA Hiroshi(*2)
MIYO Yasuhiko	MORIMOTO Masaaki(*12)	OGIWARA Norio
OKABE Tomokazu	SANO Jyunya(*6)	SANTO Masahide(*2)
SASAJIMA Tadashi	SASAKI Noboru(*2)	TAKAHASHI Shoryu(*2)
YAGYU Jun-ichi		

RF Facility Division

YAMAMOTO Takumi (General Manager)

ANNOU Katsuto	ISAKA Masayoshi	FUKUDA Hiromi (*19)
HIRANAI Shinichi	KIYONO Kimihiro	MORIYAMA Shinichi
SATO Tomio (*15)	SEKI Masami	SHIBAYAMA Minoru(*13)
SUGANUMA Kazuaki	TERAKADO Masayuki	YOKOKURA Kenji

NBI Facility Division

KURIYAMA Masaaki (General Manager)

AKINO Noboru	EBISAWA Noboru	HONDA Atsushi
ISOZAKI Nobumitsu	ITOH Takao	KAWAI Mikito
KAZAWA Minoru	MOGAKI Kazuhiko	OHGA Tokumichi
OHSHIMA Katsumi(*13)	OOHARA Hiroshi	SEKI Hiroshi(*15)
TAKAHASHI Shunji	TAKENOUCHI Tadashi(*20)	TOTUKAWA Ryoji(*13)
USUI Katsutomi	YAMAMOTO Masahiro	ZHOU Capin(*17)

JFT-2M Facility Division

TAKEUCHI Hiroshi (General Manager)(April, 1996-June, 1996)

SHIMIZU Masatsugu(General Manager)(Aug., 1996-March, 1997)

KOIKE Tsuneyuki (Deputy General Manager)

HASEGAWA Koichi	KASHIWA Yoshitoshi	KIKUCHI Kazuo
KOMATA Masao	OKANO Fuminori	OHUCHI Yutaka
SAWAHATA Masayuki	SHIBATA Takatoshi	SUZUKI Sadaaki
TANI Takashi	UMINO Kazumi(*15)	

*1 Ecole Polytechnique
*2 Hitachi Ltd.
*3 Institute of Plasma Physics Academia Sinica(China)
*4 Ioffe Physical-Technical Institute
*5 JAERI Fellowship
*6 Japan Expert Clone Corp.
*7 JST Fellowship
*8 Kaihatsu Denki Co.
*9 Kurchatov Institute
*10 Kyushu University
*11 Mito Software Engineering Co.
*12 Mitsubishi Heavy Industries, Ltd.
*13 Nippon Advanced Technology Co., Ltd.
*14 Nuclear Energy Data Center Co.
*15 Nuclear Engineering Co., Ltd.
*16 Nuclear Information Service Co.
*17 Southwestern Institute of Physics(China)
*18 STA Fellowship
*19 Sumitomo Heavy Industries, Ltd.
*20 Tomoe Shokai
*21 University of Science and Technology of China